UCRL-18178

cy. 2

University of California

Ernest O. Lawrence Radiation Laboratory

RADIOFREQUENCY RESONANCES IN MERCURY AND NEON ATOMS EXCITED BY ELECTRON IMPACT

Orilla Ann McHarris

(Ph.D. Thesis)

May 24, 1968

RECEIVED
LAWRENCE
RADIATION LABOR
JUL 1 19
LIBRARY A
DOCUMENTS S

TWO-WEEK LOAN COPY

This is a Library Circulating Copy which may be borrowed for two weeks. For a personal retention copy, call Tech. Info. Division, Ext. 5545

UCRL-18178 cy. 2

DISCLAIMER

This document was prepared as an account of work sponsored by the United States Government. While this document is believed to contain correct information, neither the United States Government nor any agency thereof, nor the Regents of the University of California, nor any of their employees, makes any warranty, express or implied, or assumes any legal responsibility for the accuracy, completeness, or usefulness of any information, apparatus, product, or process disclosed, or represents that its use would not infringe privately owned rights. Reference herein to any specific commercial product, process, or service by its trade name, trademark, manufacturer, or otherwise, does not necessarily constitute or imply its endorsement, recommendation, or favoring by the United States Government or any agency thereof, or the Regents of the University of California. The views and opinions of authors expressed herein do not necessarily state or reflect those of the United States Government or any agency thereof or the Regents of the University of California.

UCRL-18178

UNIVERSITY OF CALIFORNIA

Lawrence Radiation Laboratory
Berkeley, California

AEC Contract No. W-7405-eng-48

RADIOFREQUENCY RESONANCES IN MERCURY AND NEON ATOMS EXCITED BY ELECTRON IMPACT

Orilla Ann McHarris

(Ph.D. Thesis)

May 24, 1968

RADIOFREQUENCY RESONANCES IN MERCURY AND NEON ATOMS EXCITED BY ELECTRON IMPACT

Contents

Abstract v

I. Introduction 1

II. Theory 3

A. Alignment of the Metastable State 3

B. RF Resonance 5

C. Detection by Light Absorption 8

D. Equation for the Line 10

E. Applications 16

III. Experimental Procedure 20

A. Electron Gun 20

B. Lamp 32

C. Vacuum 33

D. Steady-State and Radio-Frequency Magnetic Fields . . . 36

E. Detection System 38

IV. Results and Discussion 41

A. Neon g_J 41

B. Mercury Lifetime 50

V. Conclusion 75

Acknowledgments 78

Appendices 79

I. Alignment Due to Cascading 79

II. The Motion of the Expectation Value of the Magnetic Moment μ 81

Footnotes and References 83

RADIOFREQUENCY RESONANCES IN MERCURY AND NEON ATOMS EXCITED BY ELECTRON IMPACT

Orilla Ann McHarris

Lawrence Radiation Laboratory
University of California
Berkeley, California

May 24, 1968

ABSTRACT

Dehmelt's technique of producing and aligning an excited atomic state by electron bombardment and then detecting an rf resonance of the state by optical means has been applied to neon for the first time. The metastable $(2^2P_{3/2}3^2S_{1/2})_2$ state was produced by collision with electrons of about 25 eV, and the resonance was detected as a change in absorption of the 6143 Å resonance radiation corresponding to a transition from the metastable state to the higher $(2^2P_{3/2}3^2P_{1/2})_2$ state. The measured g_J value agrees with that given by the atomic beam method. The magnetic field was calibrated with the rf resonance of the mercury 6^3P_2 state; this state was also produced and aligned by electron impact, and the resonance was detected as a change in absorption of the resonance radiation to the 7^3S_1 state.

In a further application of this technique, the lifetime of the mercury 6^3P_2 magnetic sublevels was obtained (as a function of the pressure of the mercury vapor). The equation for the rf resonance line was derived, and with the use of the equation the m-state lifetime was obtained both from the variation of the line width with rf power and also from the separation of the two maxima in the strongly rf-broadened

line. For pressures of 4-7 × 10^{-3} Torr the lifetime was found to be 1-0.5 × 10^{-5} sec. These values are similar to those obtained by Baumann, although in order to agree with the equation for the resonance line, his values should be multiplied by a factor of 2. The relationship of the lifetime to the most likely collision processes is discussed.

I. INTRODUCTION

An investigation was started several years ago of the potentialities of applying to the excited states of the heavier noble gases an rf resonance technique first applied by Dehmelt to mercury vapor[1] and by Lamb and Maimann to helium.[2,3] This method combines electron bombardment as a means of producing and aligning the excited state with optical detection of the rf resonance, which resonance alters the relative intensities of electric dipole transitions from the state (in both absorption and emission) by changing its alignment. The present work is a continuation of the original work[4] on the metastable $(2^2P_{3/2}3^2S_{1/2})_2$ state of neon and has been partially described in references 5 and 6. The major advantage of electron bombardment over the optical excitation used in double resonance experiments is that it can reach directly states that do not combine optically with the ground state, of which the $(2^2P_{3/2}3^2S_{1/2})_2$ state is an example. Since the lifetime of the state is relatively long (of the order of a millisecond),[4] it is possible to use the change in absorption of light corresponding to a transition to a higher excited state as a means of detecting the rf resonance; here the 6143Å resonance radiation to the $(2^2P_{3/2}3^2P_{1/2})_2$ state was used.

Since the entire atomic interaction takes place inside an electron gun, a great deal of time and effort went into the construction of a suitable gun. Optimum results were obtained from a high current-density diode operated at the lowest voltage capable of producing enough ions to neutralize the space charge. For this reason the neon resonance signal was greatly increased by adding mercury vapor to the gun. The mercury, which has a lower ionization potential than does neon, both

increased the electronic current (leading to an increase in the number of metastable atoms) and also allowed the gun to be run at a lower voltage, thus keeping the electron energies closer to the excitation threshold of the metastable state. This second condition is very important in producing a large alignment of the state.[4] The rf resonance of the mercury metastable 6^3P_2 state, observed as a change in absorption of the 5461Å line from the 6^3P_2 state to the 7^3S_1 state,[1] was first used to check the system and was later used to calibrate the field for the neon resonance.

Since the electron gun had already been constructed to handle mercury vapor, and the other equipment (such as a suitable lamp) necessary to observe the metastable mercury resonance was also available, it seemed obvious to investigate further the 6^3P_2 state. A program to measure the m-state lifetime was in progress when it came to our attention that M. Baumann had already published a very similar study in Zeitschrift für Physik.[7] Our description of the process was different, however. In particular, we had derived the equation for the resonance line, which Baumann did not do. Use of this equation leads to a factor of two difference in the expression for the lifetime and also allows one to obtain the lifetime in more than one way. In addition, our explanation for the line broadening at low pressures is different from his. Thus we feel that we still have something new to offer, and our measurement of the metastable mercury m-state lifetime will be discussed as well as the neon metastable state resonance.

II. THEORY

A. Alignment of the Metastable State

The mechanism whereby electron bombardment can align an excited atomic state at the same time that it produces the state is best described by first neglecting electron spin. In this case, if the situation is so arranged that the incoming electron has just enough energy to excite the given atomic level and have zero momentum after the collision, that electron can carry away no angular momentum (which is, after all, given by $\vec{r} \times \vec{p}$). Then the only change in the angular momentum of the atom is due to that brought in by the electron. If, however, the bombarding electron was traveling in the z direction, all its angular momentum was perpendicular to the z axis, and the angular momentum of the atom parallel to the z axis must remain unchanged. This is the same as saying that $\Delta m = 0$ for the transition; since both the neon and the mercury atoms have a ground state of $J = 0$ (and $m_J = 0$), it means that their excited states should, under these circumstances, be aligned with $m_J = 0$.

Actually, however, spin must be considered since, according to the Born-Oppenheimer theory, the excitation from a ^1S state to a ^3P state can occur only by means of electron exchange.[8,9] That is, since the wave function for collisions between identical particles must be symmetrized, just as they are for other problems involving identical particles, electron exchange is mathematically possible, and it is also physically necessary if there is to be a change in the spin of the atom: the matrix element for the transition probability is the integral of the initial states of the atom and electron, times the interaction energy

involved in the collision, times the complex conjugate of the final states, and when the very small spin-dependent forces are ignored in favor of the much larger Coulomb force, there is nothing present that can change the spin of the atom unless one of the atomic electrons exchanges places with the bombarding electron. The transition probability for the case of electron exchange is proportional to[10]

$$P(J,m \to J',m') = \left| \int d\tau_0\, d\tau_1 \cdots d\tau_n \{\chi^*(n) e^{-i\vec{k}_f \cdot \vec{r}_n} \Psi^*(J', m';0,1,\cdots n-1) \times \left[\frac{e^2}{r_{0,n}} + \frac{e^2}{r_{1,n}} + \cdots + \frac{e^2}{r_{n-1,n}} - \frac{ne^2}{r_n}\right] \chi(0) e^{i\vec{k}_i \cdot \vec{r}_0} \Psi(J,m;1,2,\cdots n)\} \right|^2$$

where $\chi(n)$ is the spin wave function of the (exchanged) outgoing electron, $\vec{k}_f$ is the wave number of the outgoing electron, $\chi(0)$ is the spin wave function of the incoming electron, and $\vec{k}_i$ is the wave number of the incoming electron.

For a bombarding electron traveling in the z direction, $e^{i\vec{k}_i \cdot \vec{r}} = e^{ik_z \cdot z}$, and at threshold excitation energy $\vec{k}_f = 0$. Thus from cylindrical symmetry the selection rule $\Delta m_L = 0$ still holds, as could also be seen from the argument in the first paragraph. $\chi(n)$ need not be the same as $\chi(0)$, however, and so Δm_S and therefore also Δm_J may be ±1 as well as zero. Δm_J may never be greater than $|1|$, though, since the transition of interest involves just one electron colliding with the atom and one electron leaving the atom. For the present cases of J = 0 ground states and J = 2 excited states, therefore, the excited state $m_J = 0, \pm 1$ levels should be populated to the exclusion of the $m_J = \pm 2$ levels. This is true for bombarding electrons at the threshold energy; at slightly higher energies $\vec{k}_f$ is still small, $e^{-ik_f \cdot r}$ is still close to unity, and

the $m_J = 0, \pm 1$ levels should still be preferentially populated by the direct excitation of the $^3P_2$ state. Of course as soon as the electron energy is great enough to populate excited states higher than the metastable state, cascading to this state must also be considered. Even this process should tend to produce alignment, however. The effect of multiple transitions on an atom entering the metastable state through a series of higher excited states is difficult to assess, but metastable atoms produced by a single downward radiative transition will definitely be aligned, as is shown in Appendix A.

Note that the z axis is fixed by the direction of the constant magnetic field in which the experiment takes place; the bombarding electrons must, therefore, travel parallel to the field axis.

B. RF Resonance

The reason for aligning the metastable atoms is so that one can notice when transitions take place among the magnetic sublevels by observing a change in the alignment. In our case, transitions from one m value to another were brought about by the well-known radio-frequency resonance method. In brief review, this means that a small, rotating magnetic field, H_r, is applied at right angles to the larger, constant field H_z, adding vectorially to it to produce a total field at an angle to, and rotating around, the z axis. To visualize what happens to an atom in this field, it is easiest to consider the equations of motion in a coordinate system rotating around the z axis with the field. In general, the motion of the magnetic moment $\vec{\mu}$ is given by

$$\frac{d\vec{\mu}}{dt} = \frac{\partial\vec{\mu}}{\partial t} + \vec{\omega} \times \vec{\mu}$$

where $\vec{\omega}$ is the angular velocity of the coordinate system. Also, equating torque with the change with time of the angular momentum,

$$\frac{d\vec{J}}{dt} = \vec{\mu} \times \vec{H} ,$$

or, since $\vec{\mu} = \gamma\vec{J}$,

$$\frac{d\mu}{dt} = \vec{\mu} \times \gamma\vec{H} .$$

Therefore, $\frac{\partial\mu}{\partial t} = \vec{\mu} \times (\gamma\vec{H} + \vec{\omega})$, so that in the rotating coordinate system $\vec{\mu}$ precesses around the effective field $(\gamma\vec{H} + \vec{\omega})$, where $\vec{H}$ is, of course, the sum of the two fields H_z and H_r. If H_r is taken, for example, along the x axis of the rotating coordinate system,

$$\frac{\partial\vec{\mu}}{\partial t} = \vec{\mu} \times (\gamma H_r\hat{i} + \gamma H_z\hat{k} + \omega\hat{k}),$$

and it is clear that when $\gamma H_z = -\omega$, the magnetic moment will be precessing around just that x axis. In the laboratory, or non-rotating, coordinate system one must, of course, include the additional motion around the z axis with frequency ω, although this cannot affect the z component of μ, which is the quantity of interest. Thus for a magnetic moment originally precessing around the z axis, the application of a magnetic field rotating at a frequency closer and closer to $(-\gamma H_z)$ will gradually tip down the axis of precession until at $\omega = -\gamma H_z$, μ has periodically a positive z and then a negative z component. Quantum mechanically the same thing happens to the expectation value of μ (see Appendix B): at $\omega = -\gamma H_z$,

$$\langle\mu_z(t)\rangle = \langle\mu_z(t=0)\rangle \cos \gamma H_r t - \langle\mu_y(t=0)\rangle \sin \gamma H_r t ,$$

and we see that for any initial orientation of μ, at resonance its expectation value in the z direction takes on, with time, its entire possible range of values.

Rabi[11] calculated explicitly, as a function of magnetic field magnitude, direction, and frequency, the probability that a spin of ½, initially in the m=+½ state with respect to the field, would, after a time t, be found in the m=-½ state with respect to the field. He found

$$P_{\frac{1}{2},-\frac{1}{2}} = [(r^2 \sin^2 \theta)/(r^2+\nu^2-2\nu r \cos \theta)] \sin^2[\pi + (r^2+\nu^2-2\nu r \cos \theta)^{\frac{1}{2}}]$$

where $r = \omega/2\pi$ is the frequency of rotation of the magnetic field, θ is the angle between the total field and the axis about which it is rotating and ν is the Larmor frequency. For the angular momentum quantized along the z axis rather than along the total magnetic field, $P_{\frac{1}{2},-\frac{1}{2}}$ takes its more usual form[12,13]

$$P_{\frac{1}{2},-\frac{1}{2}} = \frac{(\omega_0 H_1/H_0)^2}{(\omega_0-\omega)^2 + (\omega_0 H_1/H_0)^2} \sin^2 \left[\frac{t_2-t_1}{2} ([\omega_0-\omega]^2 + [\gamma H_1]^2)^{\frac{1}{2}}\right],$$

where H_0 is the constant field in the z direction, $\omega_0/2\pi$ is the Larmor frequency, and H_1 is the magnetic field which rotates around the z axis with angular velocity ω and which was turned on at time t_1 and turned off at time t_2. The probability that an atom originally in an m state will later be found in an m' state can be extended to cases in which the angular momentum J is greater than ½ by applying a formula due to Majorana:[14]

$$P(J,m,m',t) = (\cos\tfrac{\alpha}{2})^{4J}(J+m)!(J-m)!(J-m')!(J+m')!$$
$$\times\left[\sum_{n=0}^{2J}\frac{(-1)^n}{n!(n-m+m')!(J+m-n)!(J-m'-n)!}(\tan\tfrac{\alpha}{2})^{2n-m+m'}\right]^2 ,$$

where $\sin^2 \alpha/2 = P_{\frac{1}{2},-\frac{1}{2}}$ calculated in the appropriate coordinate system.

Thus, as the frequency of rotation of H_r is varied from a value on one side of the Larmor frequency, through the Larmor frequency, to a value on the other side of it (or, alternatively, if the Larmor frequency is varied by slowly changing the magnitude of the "constant" field in the z direction), the transition probabilities pass through their maximum amplitudes, and the resonance line for transitions from one m state to another is swept out. This line can be drawn by a changing absorption of linearly polarized light whose wave length corresponds to a transition to a higher excited state:

C. Detection by Light Absorption

For the absorption of light polarized along the z axis, the possible transitions and relative transition probabilities between the $^3S_1$ and metastable $^3P_2$ states in mercury and the $(2^2P_{3/2}3^2P_{1/2})_2$ and metastable $(2^2P_{3/2}3^2S_{1/2})_2$ states in neon are those diagrammed in Figs. 1a and 1b. When the metastable mercury atoms are aligned, essentially every metastable atom is able to absorb the polarized 5461 Å light, but as the field H_r rotates at a frequency closer and closer to the Larmor frequency, more and more metastable atoms are transferred to the m=±2 states, from which they cannot be optically excited to the $^3S_1$ state with linearly polarized light. Therefore the mercury radio-frequency resonance line is reproduced as a decrease in the absorption of the 5461 Å light. When the metastable neon

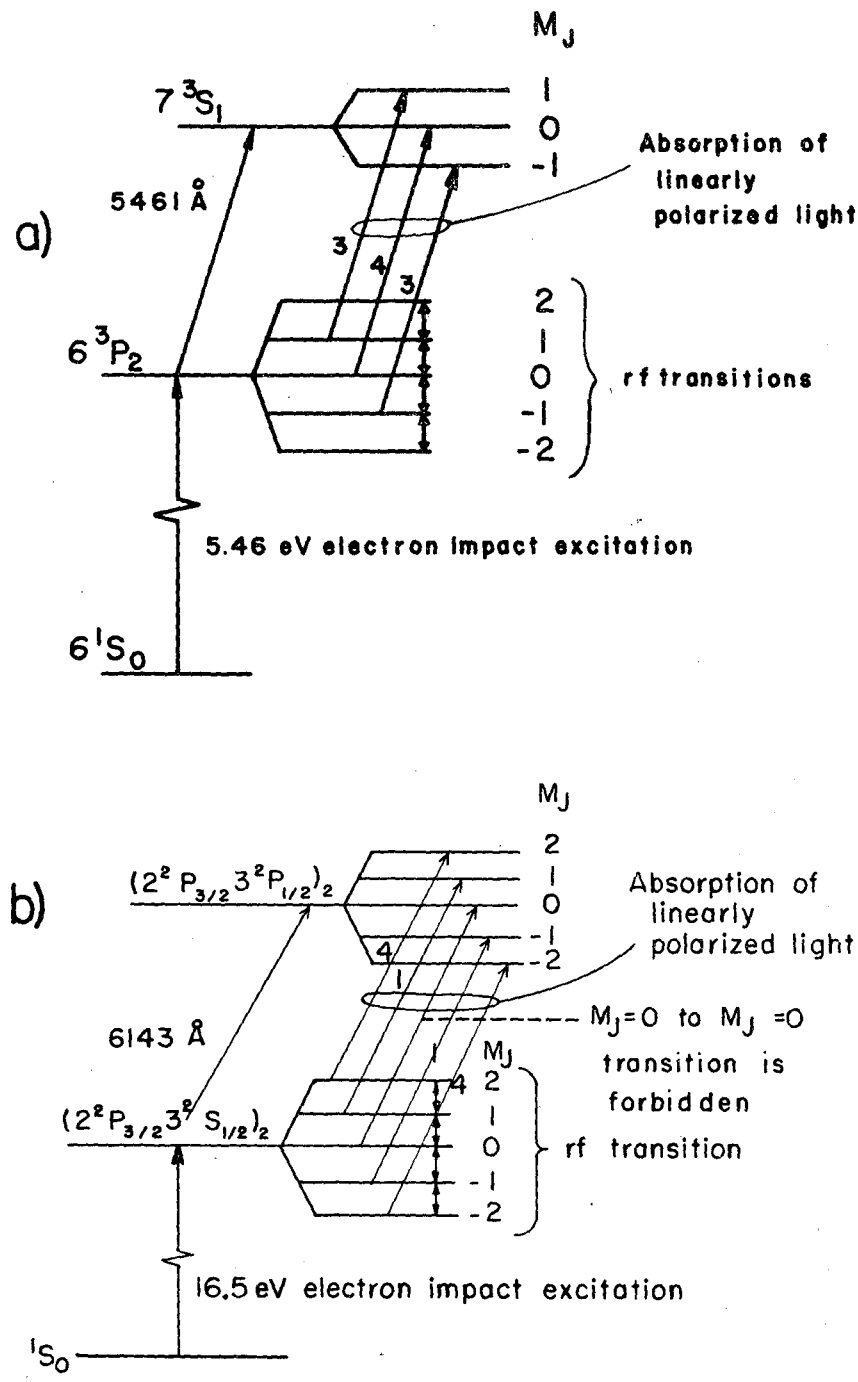

XBL 684-707

Fig. 1. The energy levels involved in the rf resonances of metastable mercury (a) and neon (b).

atoms are aligned, only those in the m=±1 states can absorb the polarized 6143 Å light in a transition to the higher excited state (note that a $\Delta m_J=0$, $\Delta J=0$ transition is forbidden); as the m=±2 states are populated by the rotating magnetic field, however, more and more atoms are in a condition to absorb the resonance radiation, and the neon radio-frequency resonance line is displayed as an increase in the absorption of the 6143 Å light.

D. The Equation for the Line

With the use of the optical transition probabilities and the Rabi-Majorana formula for $P(J,m,m',t)$, the equations for these resonance lines can be derived. For the case of mercury we know that at a time t very soon after t_i, the time at which a particular group of atoms was raised to the metastable state, the amount of linearly polarized light absorbed by those atoms is

$$A(t-t_i) \propto 4n_0(t)+3n_1(t)+3n_{-1}(t), \text{ where}$$

$$n_0(t) = \text{the population of state } m=0 \text{ at time } t$$

$$= \delta n_0(t_i)[1-2P(2,0,1,t-t_i)-2P(2,0,2,t-t_i)]+2\delta n_1(t_i)P(2,1,0,t-t_i)$$
$$+2\delta n_2(t_i)P(2,2,0,t-t_i), \text{ and}$$

$$n_{-1}(t) = n_1(t) = \delta n_1(t_i)[1-P(2,1,0,t-t_i)-P(2,1,2,t-t_i)-P(2,1,-2,t-t_i)]$$
$$+\delta n_0(t_i)P(2,0,1,t-t_i)+\delta n_{-2}(t_i)P(2,-2,1,t-t_i)$$
$$+\delta n_2(t_i)P(2,2,1,t-t_i).$$

Here $\delta n_0(t_i)$ $[\delta n_1(t_i), \delta n_2(t_i)]$ is the number of atoms raised to the m=0 [m=±1, m=±2] sublevel of the metastable state at t_i. $\delta n_{-1}(t_i)=\delta n_1(t_i)$ since the cross section for the production of m=-1 is the same as for

m=1 (see the expression for the matrix element for the transition probability due to electron bombardment). In addition, $P(J,m,m',t)$ is symmetric in m and m', and $P(J,m,m',t) = P(J,-m,m',t)$ whenever $|m-m'| = |-m-m'|$. Equal terms have therefore been combined, and populations symmetric in m and -m set equal: $\delta n_2=\delta n_{-2}$, $n_1=n_{-1}$, and $n_2=n_{-2}$, as well as $\delta n_1=\delta n_{-1}$.

The change in absorption produced by the rotating field is, then

$$\begin{aligned}\Delta A_{t-t_i} \propto\ & 4\{-\delta n_0(t_i)[2P(2,0,1,t-t_i)+2P(2,0,2,t-t_i]+2\delta n_1(t_i)P(2,0,1,t-t_i) \\ & +\delta n_2(t_i)P(2,0,2,t-t_i)\}+6\{-\delta n_1(t_i)[P(2,0,1,t-t_i)+P(2,1,2,t-t_i) \\ & +P(2,1,-2,t-t_i)]+\delta n_0(t_i)P(2,0,1,t-t_i)+\delta n_2(t_i)[P(2,1,2,t-t_i) \\ & +P(2,1,-2,t-t_i)]\} \text{ , or}\end{aligned}$$

$$\begin{aligned}\Delta A_{t-t_i} \propto\ & P(2,0,1,t-t_i)[-2\delta n_0(t_i)+2\delta n_1(t_i)]+P(2,1,2,t-t_i)[-6\delta n_1(t_i)+6\delta n_2(t_i)] \\ & +P(2,0,2,t-t_i)[-8\delta n_0(t_i)+8\delta n_2(t_i)]+P(2,1,-2,t-t_i)[-6\delta n_1+6\delta n_2] \ .\end{aligned}$$

Actually, however, the metastable state was continuously produced for all $t_i<t$, so the expression really needed is (omitting the factor of two)

$$\begin{aligned}\Delta A \propto & \int_{-\infty}^{t} dt_i \left\{P(2,0,1,t-t_i)\left[\frac{dn_1}{dt_i}-\frac{dn_0}{dt_i}\right]+3P(2,1,2,t-t_i)\left[\frac{dn_2}{dt_i}-\frac{dn_1}{dt_i}\right]\right. \\ & \left. +4P(2,0,2,t-t_i)\left[\frac{dn_2}{dt_i}-\frac{dn_0}{dt_i}\right]+3P(2,1,-2,t-t_i)\left[\frac{dn_2}{dt_i}-\frac{dn_1}{dt_i}\right]\right\} \\ = & \int_{0}^{\infty} dt \left\{P(2,0,1,t)\left[\frac{dn_0}{dt}-\frac{dn_1}{dt}\right]+3P(2,1,2,t)\left[\frac{dn_1}{dt}-\frac{dn_2}{dt}\right]+4P(2,0,2,t)\right. \\ & \left.\left[\frac{dn_0}{dt}-\frac{dn_2}{dt}\right]+3P(2,1,-2,t)\left[\frac{dn_1}{dt}-\frac{dn_2}{dt}\right]\right\} \ .\end{aligned}$$

$$\Delta A \propto 6(r_0+r_1-2r_2) \int_0^\infty dt \left\{ \sin^2 \frac{\alpha}{2} - \sin^4 \frac{\alpha}{2} \right\} e^{-(G+2g)t} \quad .$$

(Here we see that, as one would expect, the change in absorption of the light due to the rotating field would be zero if $r_0=r_1=r_2$; i.e. if there were no population difference created by the electron bombardment.)

Writing

$$\sin^2 \frac{\alpha}{2} = \frac{(\gamma H_r)^2}{(\omega-\omega_0)^2 + (\gamma H_r)^2} \sin^2 \left[\frac{t}{2} \sqrt{(\omega-\omega_0)^2 + (\gamma H_r)^2} \right] \quad ,$$

for quantization along the z axis, and integrating, we have finally,

$$\Delta A \propto \frac{3(r_0+r_1-2r_2)(\gamma H_r)^2}{G+2g} \left\{ \frac{1}{(G+2g)^2+(\gamma H_r)^2+(\omega-\omega_0)^2} - \frac{3(\gamma H_r)^2}{[(G+2g)^2+(\gamma H_r)^2+(\omega-\omega_0)^2][(G+2g)^2+4(\gamma H_r)^2+4(\omega-\omega_0)^2]} \right\} \quad .$$

For the case of neon, the amount of 6143 Å light absorbed is

$$A_{Ne}(t-t_i) \propto n_1(t)+n_{-1}(t)+4n_2(t)+4n_{-2}(t) \quad .$$

The expressions for the $n_j(t)$ are the same as in the calculations for mercury since there are again five m states; as before we will want to integrate all time $t_i<t$; and, in addition, the expressions for the $\frac{dn_j}{dt}$ will be the same as for mercury since there are again two lifetimes. We have, therefore,

$$\Delta A_{Ne}(t-t_i) \propto 2P(2,1,0,t-t_i)[-\delta n_1+\delta n_0]+2P(2,1,2,t-t_i)[-\delta n_1+\delta n_2]$$
$$+2P(2,-2,1,t-t_i)[-\delta n_1+\delta n_2]+8P(2,2,0,t-t_i)[-\delta n_2+\delta n_0]$$
$$+8P(2,1,2,t-t_i)[-\delta n_2+\delta n_1]+8P(2,-2,1,t-t_i)[-\delta n_2+\delta n_1] \text{ , or}$$

$$\Delta A_{Ne} \propto \int_0^\infty dt\{P(2,1,0,t)[r_1-r_0]+3P(2,1,2,t)[r_2-r_1]$$
$$+4P(2,2,0,t)[r_2-r_0]+3P(2,-2,1,t)[r_2-r_1])e^{-(G+2g)t}\} \quad .$$

Without preceeding any further, we can at this point see that ΔA_{Ne} is going to be exactly the negative of ΔA in the mercury calculation, indicating that the general line shapes should be identical, although one goes through a maximum and the other through a minimum, and although the actual height (or depth) of the lines depends on the relationships among the r's and on the proportionality factors.

Brossel and Bitter[15,16] obtained essentially the same expression for the atomic radio-frequency resonance of the $^3P_1$ state in mercury. The factor involving the r's would, of course, be different, and the only lifetime in their expression is the very short one of the P_1 state itself, but the somewhat surprising thing is that even here the integral is the same. In the J=2 case, the additional higher powers of sin $\alpha/2$ introduced by the $(\cos \alpha/2)^{4J}$ factor in the Majorana transition probability are exactly canceled by the (solely higher order) terms introduced by including the transitions for m>1. The general line shapes appear therefore to be the same whether J=1 or 2, and whether the excited state is metastable or not, even though for any given resonance the lifetime term has its own form and the height of the line depends on the factor in front of the

integral: the differences in excitation rates, and also the incident light intensity and the absolute optical transition probabilities.

E. Applications

The metastable state g_J value is the most obvious quantity derivable from these radio-frequency resonances since at resonance (for an even isotope) $\omega=\omega_0=g_J\mu_0H_z/\hbar$, or $g_J=\hbar\omega_0/\mu_0H_z$ in terms of known and experimental quantities. This was already clear from the original discussion of a spin in a rotating magnetic field, and it re-appears in the equation for the resonance line, which can be seen to be a maximum at $\omega=\omega_0$.

The other metastable-atom characteristic we looked for was the lifetime of the m-states in mercury. This is 1/g (assuming a uniform relaxation rate) in the equation for the line, and it clearly affects the resonance because inelastic collisions among the atoms will re-orient them even in the absence of the rf field. Since the metastable-state lifetime is relatively long, it should be the m-state lifetime that really determines the width of the resonance line. The lifetime and half-width can be related by the use of the equation for the line. The resonance at maximum is

$$\Delta A_{max} = C\left\{\frac{(\gamma H_r)^2}{(G+2g)^2+(\gamma H_r)^2} - \frac{3(\gamma H_r)^4}{[(G+2g)^2+(\gamma H_r)^2][(G+2g)^2+4(\gamma H_r)^2]}\right\},$$

and if $\Delta\omega$ is half the line width at half maximum $[(\omega_{half}-\omega_0)=\Delta\omega]$,

$$\tfrac{1}{2}\Delta A_{max}=C\left\{\frac{(\gamma H_r)^2}{(G+2g)^2+(\gamma H_r)^2+(\Delta\omega)^2} - \frac{3(\gamma H_r)^4}{[(G+2g)^2+(\gamma H_r)^2+(\Delta\omega)^2][G+2g)^2+4(\gamma H_r)^2+4(\Delta\omega)^2]}\right\}$$

$$=\tfrac{1}{2}C\left[\frac{(\gamma H_r)^2}{(G+2g)^2+4(\gamma H_r)^2}\right] .$$

Here (G+2g) is the only quantity which is not, in theory at least, measurable. In practice H_r, the strength of the rotating magnetic field, is very difficult to measure. In the end what we did was to measure the approximate current going into the H_r loops at a point very close to the loops. Then the approximate field strength can be calculated, and the equation for the lifetime can be used in either of two different ways.

In the limit of zero rf field, the width of the resonance line should be due entirely to its finite lifetime: $\Delta\omega=1/\tau$. This is a very convenient relationship, because one does not have to know the strength of the rf field in order to be able to use it. Since, however, one does not, in this method, observe a resonance unless one applies an rf field, what can be done is to measure the line width at gradually decreasing rf field amplitudes and then extrapolate to zero field in order to find the lifetime or, in our case, combination of lifetimes. From the equation for the line the half width can be obtained as a function of the rf power at small rf amplitudes. If we solve for $(\Delta\omega)^2$ in the above equation, we find

$$(\Delta\omega)^2 = \frac{1}{8}\left\{3(G+2g)^2+24(\gamma H_r)^2+\sqrt{25(G+2g)^4+224(G+2g)^2(\gamma H_r)^2+640(\gamma H_r)^4}\right\}$$

For $(\gamma H_r)/(G+2g)$ small, this can be expanded as

$$(\Delta\omega)^2 \approx \frac{1}{8}\left\{3(G+2g)^2+24(\gamma H_r)^2+5(G+2g)^2\left[1+\frac{224}{50}\left(\frac{\gamma H_r}{G+2g}\right)^2\right]\right\} \quad \text{, or}$$

$$(\Delta\omega)^2 \approx (G+2g)^2+5.8(\gamma H_r)^2 \quad .$$

Thus $(\Delta\omega)^2$ plotted as a function of $(\gamma H_r)^2$ should follow a straight line whose intercept with the y axis is $(G+2g)^2$. Brossel and Bitter checked the form of this expression against their experimental results for the $^3P_1$ states in mercury and found it to hold true even to the numerical coefficient, 5.8 .

Another way to make use of the equation for the resonance line is to consider pairs of $(H_r,\Delta\omega)$ measurements. The measured current into the rf loops was only approximate because it was recorded as the voltage drop across a resistor, and at the frequencies involved (7-8 Mc/sec) and the small resistance (0.9 Ω) necessary in order not to reduce the rf power too much, the a.c. impedance of the resistor may have been almost twenty times its d.c. resistance. In addition, even if the current had been measured exactly, it would have been difficult to be certain that it was the same current that was present in the rf loops; it was undesirable to make the measurements in the loops themselves as all efforts had been made to reduce as much as possible the voltage drop across the loops, so as to avoid discharging the gas inside the electron gun. Approximate as the current measurements may have been, however, they were all made in exactly the same fashion for each run, so that it seemed fair to say that $H_r=kH_r'$ where H_r' is the calculated field and k is a constant for any set of the measurements. Then k can be eliminated between each two pairs of $(H_r',\Delta\omega)$ measurements and a value of (G+2g) calculated for each set of pairs. Since 1/G, the lifetime of the metastable state, has been measured for mercury, one can end up with values for g, the reciprocal of the m-state lifetime, but as we shall see, g is the more effective

quantity by at least an order of magnitude, so it may not be significant to subtract out G anyway. The final equation to be solved would be, then,

$$\left[\frac{(H_r')_1}{(H_r')_2}\right]^2 = \frac{-5(G+2g)^2-24(\Delta\omega_1)^2+\sqrt{9(G+2g)^4+640(\Delta\omega_1)^4+192(G+2g)^2(\Delta\omega_1)^2}}{-5(G+2g)^2-24(\Delta\omega_2)^2+\sqrt{9(G+2g)^4+640(\Delta\omega_2)^4+192(G+2g)^2(\Delta\omega_2)^2}} \quad .$$

Actually, a variant of this equation was used for what were the most extensive measurements. The Rabi-Majorana formula was derived exactly, not as the result of perturbation theory or any approximations. Thus it holds true even for large values of H_r, in particular for rotating fields strong enough to cause at resonance a double change in m, for example from an optically absorbing state, to a non-absorbing state, and back to an absorbing state again. When this happens, the resonance line has two maxima separated by a minimum at $\omega=\omega_0$. The points where an experimental curve is at a maximum are often easier to pick out than half-widths are, especially if there is any background which can obscure the true height of a line. We made use of this effect, therefore, to obtain values for (G+2g) from the equation for the maxima of the rf-broadened resonance line:

$$(\gamma H_r)^2 = \frac{1}{16}\left\{8(\omega_m-\omega_0)^2-7(G+2g)^2+3\sqrt{9(G+2g)^4+64(\omega_m-\omega_0)^4+16(G+2g)^2(\omega_m-\omega_0)^2}\right\} \quad .$$

Again pairs of (H_r', $|\omega_m-\omega_0|$) measurements were used in order to avoid having to know H_r exactly.

III. EXPERIMENTAL PROCEDURE

A. Electron Gun[17]

Figure 2 is a block diagram of the experimental set-up. It is inside the electron gun that the atomic interaction takes place, and a great deal of effort was devoted to its construction. There are a number of requirements that must be met: The electrons must travel in straight lines in the z direction in order to produce aligned metastable atoms, and to the same purpose they must carry at least the excitation energy, but if possible no more. The current should be relatively large in order to produce as many metastable atoms as possible (without, however, discharging the gun or creating a magnetic field that would interfere with the experiment), but the electrode spacing must be such that there is room for the beam of light to pass through that part of the gun in which the metastable atoms are being created. In addition, the parts must all be non-magnetic, since the experiment takes place inside a magnetic field. (We used nickel as a base for our oxide-coated cathodes, but when in operation, the cathode is heated well above the Curie point.) Also in order not to distort the applied magnetic field any field due to the cathode heater must be eliminated; we always wound the heater wire "non-magnetically", but that did not completely do away with its effect (see below).

It was at first thought that a relatively big electron gun was necessary in order to produce a signal large enough to be observable. That is, it appeared from the original experiments on neon that the best way to increase the too-small signal-to-noise ratic would be to increase

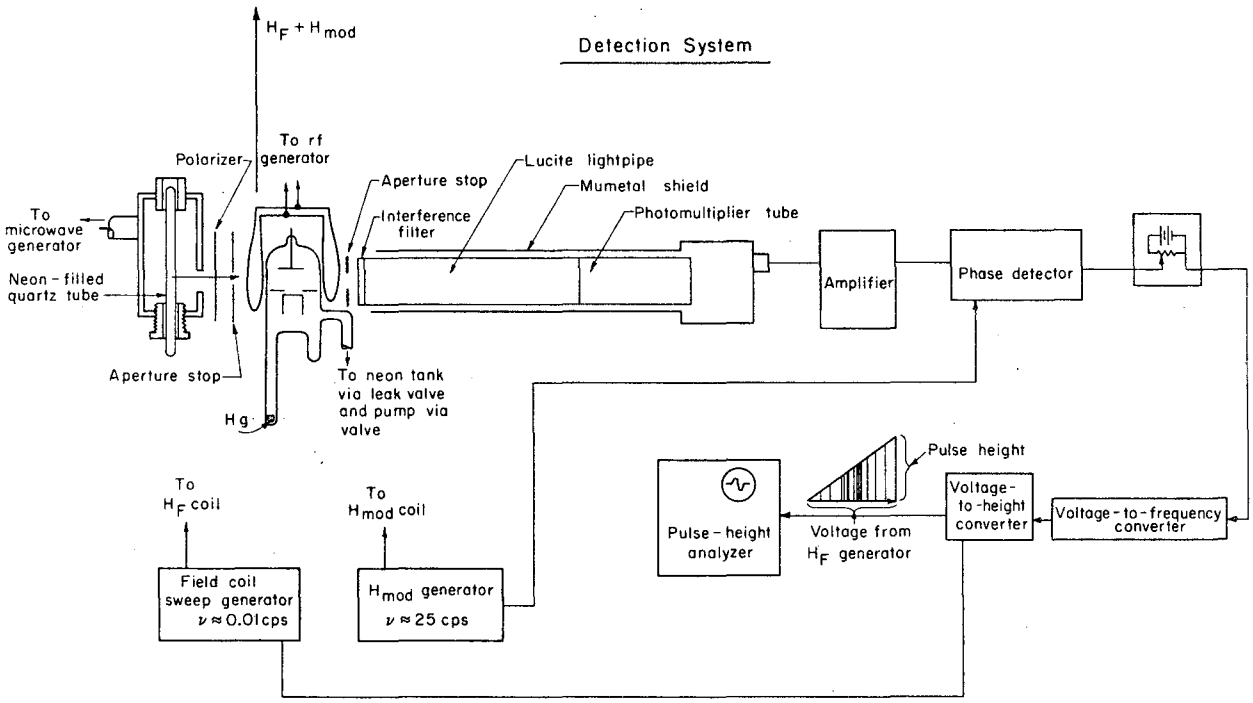

MUB-4325

Fig. 2. A block diagram of the experimental arrangement. The particular case pictured is that of a neon resonance for which an a.c. resonance signal was obtained by modulating the "constant" magnetic field in the z direction. For the case of modulation of the rf field, the only changes would be the elimination of the H_{mod} coil, the substitution of the rf modulation for the main field modulation as the reference frequency for the phase detector, and the substitution of a normal line shape for the dispersion-shape curve pictured at the pulse height analyzer.

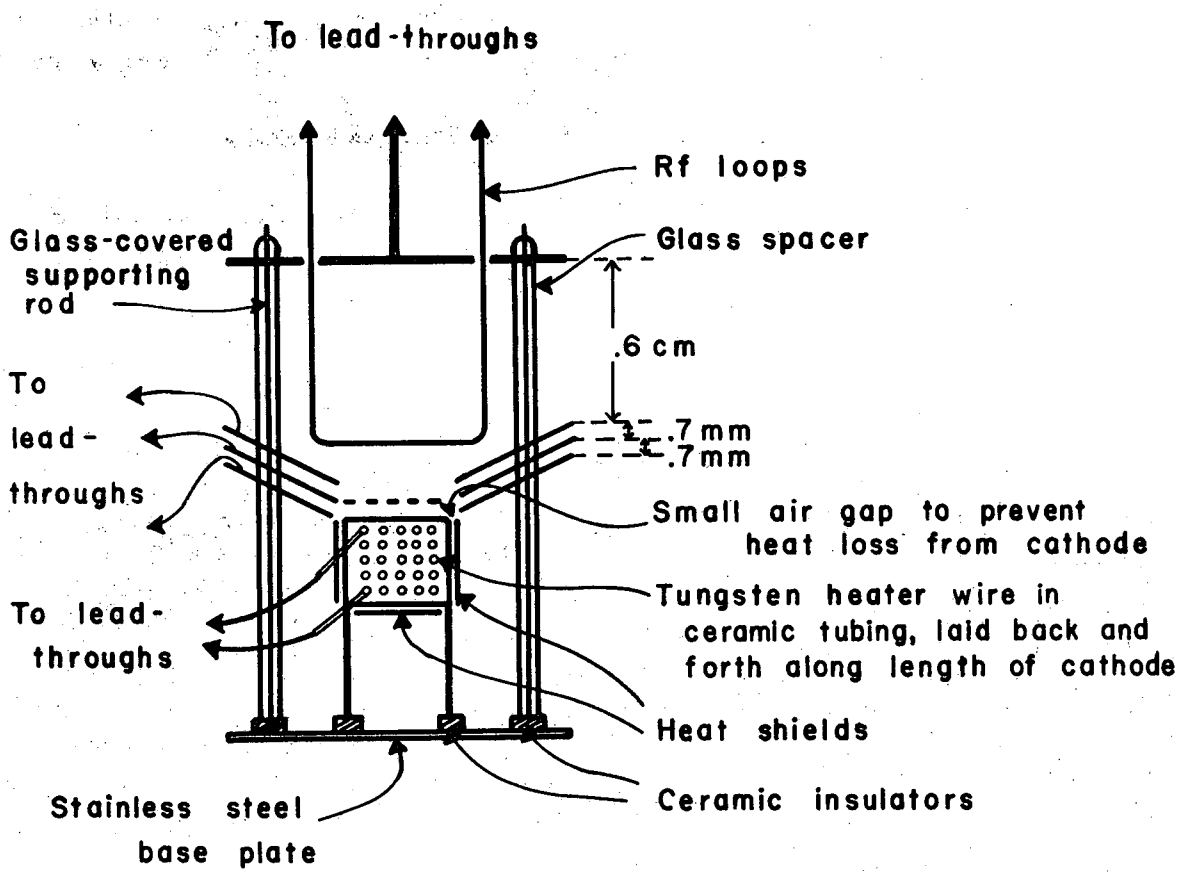

XBL 684-437

Fig. 3. End view of one of the modified Pierce-type electron guns. This gun had a rectangular, 10 cm x 1.5 cm, oxide-coated cathode. Because of its size, it was mounted directly into a stainless steel arm of the vacuum system; the two end walls were, however, of glass so that the monitoring light could pass through. Electrical connections were made by means of insulated lead-throughs. Notice that in this case the rf loop was built right into the gun.

Electron Gun

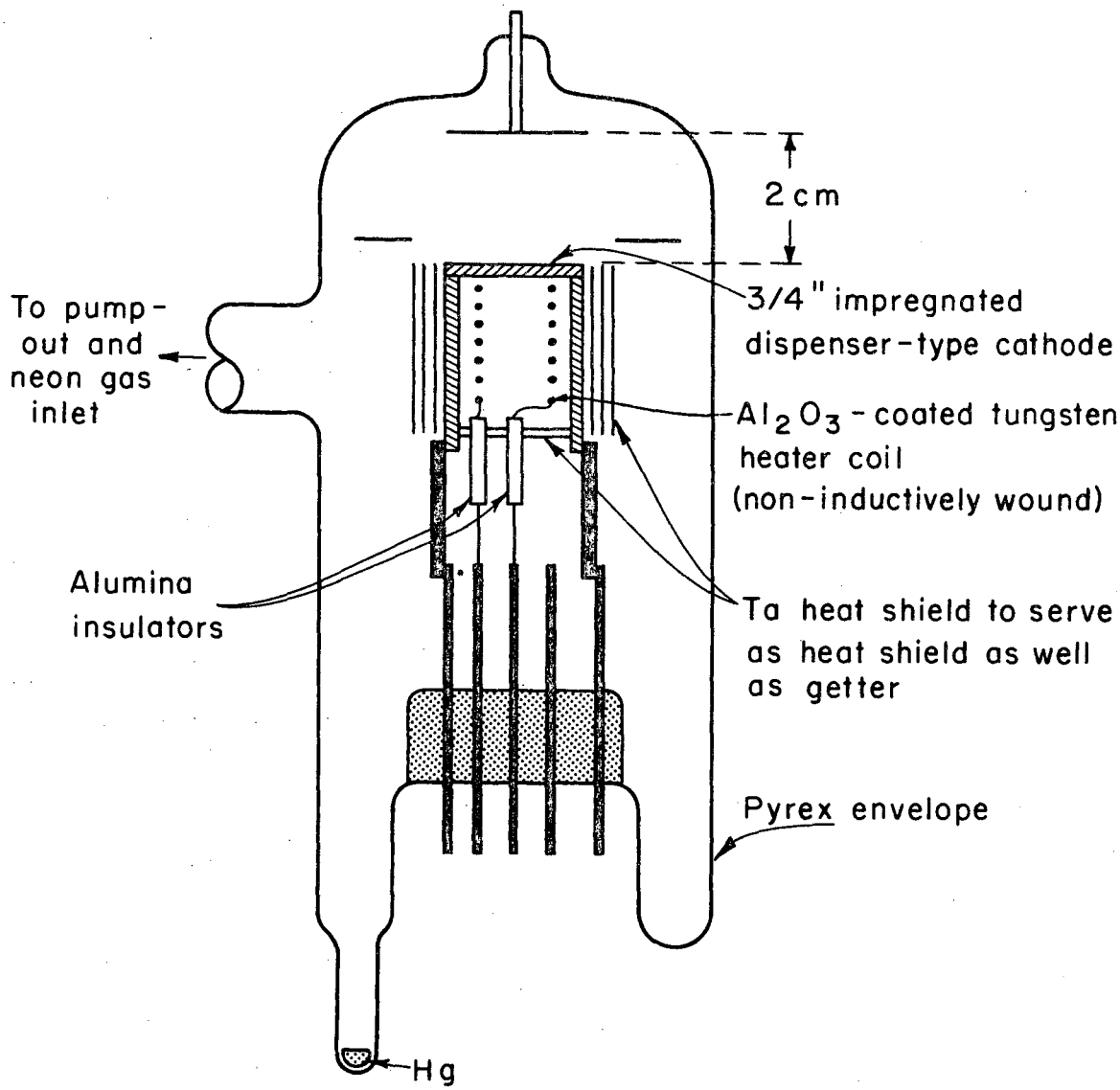

MUB-4324

Fig. 4. Electron gun with dispenser-type cathode. This particular version has an aperture ring close to the cathode to eliminate any edge effect by stopping those electrons that might leave the cathode at an angle to the z axis. This component was not included in the later guns; in those the heat shield came up very slightly higher and seemed to perform the same function.

as much as possible the path length of the resonance light through the gun, thereby increasing the optical absorption and thus also the signal at the photomultiplier. Sone of the early guns had, therefore, rectangular cathodes 10 cm × 1.5 cm . These cathodes were of nickel which was either spray-coated with what became, after activation, an emitting oxide or which was covered with a commercial thin film which similarly could be made to form an emitting surface. Most of these guns were triodes, with a modified Pierce[18] configuration (the electrodes in a true Pierce gun should lie along the calculated equipotential surfaces, but in our tubes the cathode and grid deflectors were parallel because of the difficulties involved in making accurately angled spacers for the 1 mm or so gap in question, and also the anode was usually flat for ease of construction.) The biggest problem was to make grids that would not, under operating temperatures, expand to the point where they would sag down and cause a short circuit to the cathode, but another very great disadvantage of these guns was the destructibility of the oxide-coated cathodes. Once activated, they are extremely sensitive to water vapor, organic vapors, and positive ion bombardment, all of which means that they poison easily and in addition have to be replaced every time the tube is opened to correct any other malfunction.

The use of tungsten dispenser cathodes made the construction of the electron guns very much easier. This kind of cathode is made of a refractory metal with an inset on the top of partially-sintered tungsten impregnated with a material which is a good electron emitter, in our case barium oxide. To activate the cathode, it is gradually heated to

1190° C; this drives some of the barium oxide to the top of the porous tungsten, where it forms the emitting surface. The cathodes are quite durable and can even be exposed to air and re-activated several times over; they also are reported to be capable of emission up to about 10 amp/cm^2 with a long life, though we never operated ours at that high a current density.

We were able to use these hardier, commercially produced cathodes as soon as it was determined that the long path length for optical absorption was not absolutely necessary in order to obtain a measurable signal. (We nevertheless used the largest cathode available; it had a circular surface 3/4 in. in diameter.) This came about partly as the result of an improved detection system and partly as the result of adding mercury vapor even to the neon-filled tubes. The mercury ionizes readily, and the ions, being heavy, do not immediately move to the cathode. Thus the space charge is effectively neutralized throughout the tube, except for the small region just above the cathode; electrons leaving the cathode experience essentially their entire acceleration in the first 0.5 mm or so, and from there on "coast" through the field-free region to the anode.[19] A grid is not necessary under these conditions, and so the construction of the gun was simplified even further, to a diode configuration. Among the advantages of the space charge neutralization condition are these: the electrons move in quite straight lines in the z direction due to their rapid acceleration in the direction perpendicular to the cathode surface and their subsequent motion through the field-free region to the anode (one can see this, since the cylindrical volume

between cathode and anode through which the electrons pass is more brightly lit than the rest of the tube), whereas in a triode the electrons may focus or defocus, depending on the relationship of the grid and plate voltages; the large field-free region in which the electrons have their maximum energy offers to the incoming light beam a large cross section in every part of which metastable atoms exist; and, most important, a reasonable current is possible at lower plate voltages and gas pressures.

These dispenser-type cathodes were bought sealed in glass but unactivated, and the tubes were constructed at the laboratory. Making the heater was the most critical operation, as the cathodes are heavy and have a large heat capacity, while at the same time the heater current that could be used was limited by the temperature of the wire compared to the rated maximum working temperature (1400°C) of the alumina insulation. Twenty mil tungsten wire, as long as could be coiled into the cathode, was (non-magnetically) wound on a jig of the appropriate size and shape. To outgas and anneal it, it was fired in a hydrogen atmosphere at about 900°C for approximately 5 minutes; after this the wire holds its shape but is extremely brittle. The alumina insulation was deposited on the wire by electrolysis. By thoroughly heat-shielding the sides and bottom of the cathode, it could be held at operating temperature, about 1025°C, by a current of about 4.5 amp. According to Fig. 5 this implies a temperature of about 1000°C for an uninsulated tungsten wire in a vacuum, and we hoped that our coiled and insulated wire would therefore be at something less that 1400°C. Nevertheless, a blackish deposit formed with use on the gun's glass envelope in the

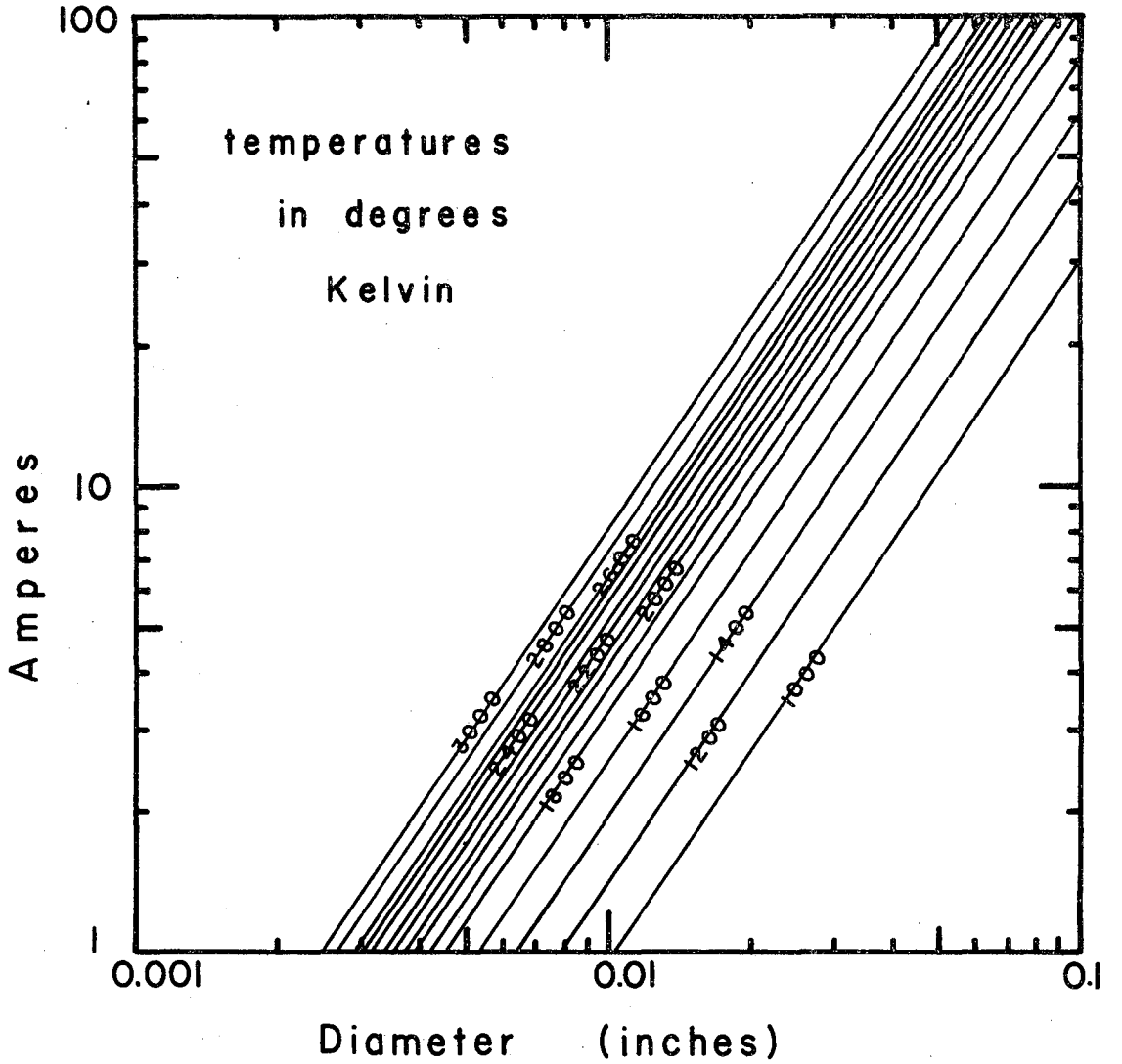

XBL 684-438

Fig. 5. "Amperes versus Wire Size for Tungsten Filaments", from George Becker, Electrical Engineering Department, University of California at Berkeley.

neighborhood of the cathode, and there is considerable evidence (see Section IV.B) that the heater wire was still too hot, causing the alumina to boil off. The heater was always constructed to be at a floating potential so that if at any point it accidentally became shorted to the cathode, it would still operate.

The anode was made of molybdenum, which does not tend to outgas or to amalgamate with mercury; it was circular and 3/4 in. in diameter like the cathode and was spaced 2 cm from the cathode. Tungsten leads were spot welded to the electrodes (with platinum as "flux" in the case of the purely neon-filled tubes but with just a relatively heavy-duty spot welder for the tubes which were to have mercury in them, since mercury amalgamates with platinum) and came out of the tube through a uranium glass press. The envelope was about 10 cm high and 4.5 cm in diameter: with these dimensions, the time between disorienting wall collisions for a mercury atom should be enough longer than the time between disorienting collisions with other atoms that it can be ignored in the calculations of the m-state lifetimes.

In order to be able to control the pressure of the mercury vapor in the electron guns, the tubes were built with a long glass side-arm, the temperature of which could be controlled independently of the temperature in the gun. A few drops of mercury were enclosed in a small, evacuated, glass capsule with a thin, easily broken neck. This capsule was placed in the side-arm with a small magnet on top of it. After the cathode was activated, the mercury could be let into the gun by breaking open the capsule with the magnetic hammer. When the tubes were to have neon in them, a commercial bottle of reagent-grade neon was connected to the

vacuum system but separated from the gun by valves that allowed it to be introduced into the gun slowly, after activation. Since neon is not affected by getters, the tubes that had only neon in them were built to include barium getters; the tubes that contained mercury did not have getters.

When the gun was entirely assembled on the vacuum system, the gun, ionization gauge, and cold trap were thoroughly outgassed by baking under vacuum for several hours or until, when the system had cooled down and the liquid nitrogen trap was filled, the pressure was approximately 10^{-8} Torr. The cathode was then activated, and the metal parts were again outgassed by induction heating. The tubes that were used for making the g_J measurements usually remained on the vacuum system so that it was possible to change the neon pressures and to switch back and forth between mercury and neon measurements just by pumping out between runs. (Also, of course, the gun stays cleaner that way.) The tubes that were used for the lifetime measurements were usually sealed off and removed from the vacuum system, since in those measurements the pressure was changed just by heating or cooling the mercury, and it was more convenient to enclose the gun in an oven when it was portable.

Typical running conditions for our modified Pierce-type guns with just neon in them were: plate voltage 42 V, grid voltage 22 V, and plate current 650 mA, at a pressure of 7 microns. A diode with a dispenser-type cathode filled with 12 microns of neon and 1 micron of mercury was operated at a plate voltage of 27.5 V and current of 50 mA; with 12 microns of neon and 9 microns of mercury, the same gun was operated at 21 V and 50 mA. The diodes with just mercury in them were

run at 11.3 V and 200 mA, at a pressure of 1.3×10^{-3} Torr, to 7.9 V and 200 mA, at a pressure of 7.1×10^{-3} Torr.

The mercury-filled guns for the lifetime measurements were enclosed, except for the sidearms containing the liquid mercury, in aluminum boxes lined with asbestos; the metal box provided shielding from stray r-f fields, while the heat insulation kept the entire gun, heated by its own cathode, at a temperature well above the highest temperature to which the liquid mercury was ever raised. Under this condition, the pressure of the mercury in the gun was the vapor pressure corresponding to the temperature of the liquid mercury in the sidearm. This latter was immersed in water and its temperature controlled by the temperature of the water, which was heated with electric immersion heaters and kept stirred by a constant flow.

Although the cathode heater wire was always wound "non-magnetically", there was apparently a residual magnetic field due to it; the interaction region is, after all, right next to the cathode. When we took runs with the heater current pulsed at 50 cps and the detection system gated to operate only in those half cycles when the heater was off, the width of the resonance line was noticeably smaller than when the heater was on all the time. As an example, see Fig. 6, which shows several resonances displayed as the first derivative of the resonance line. The expression for the relationship between the line width and the distance between the points of inflection is very complicated in general, but for small rf field amplitudes one can write

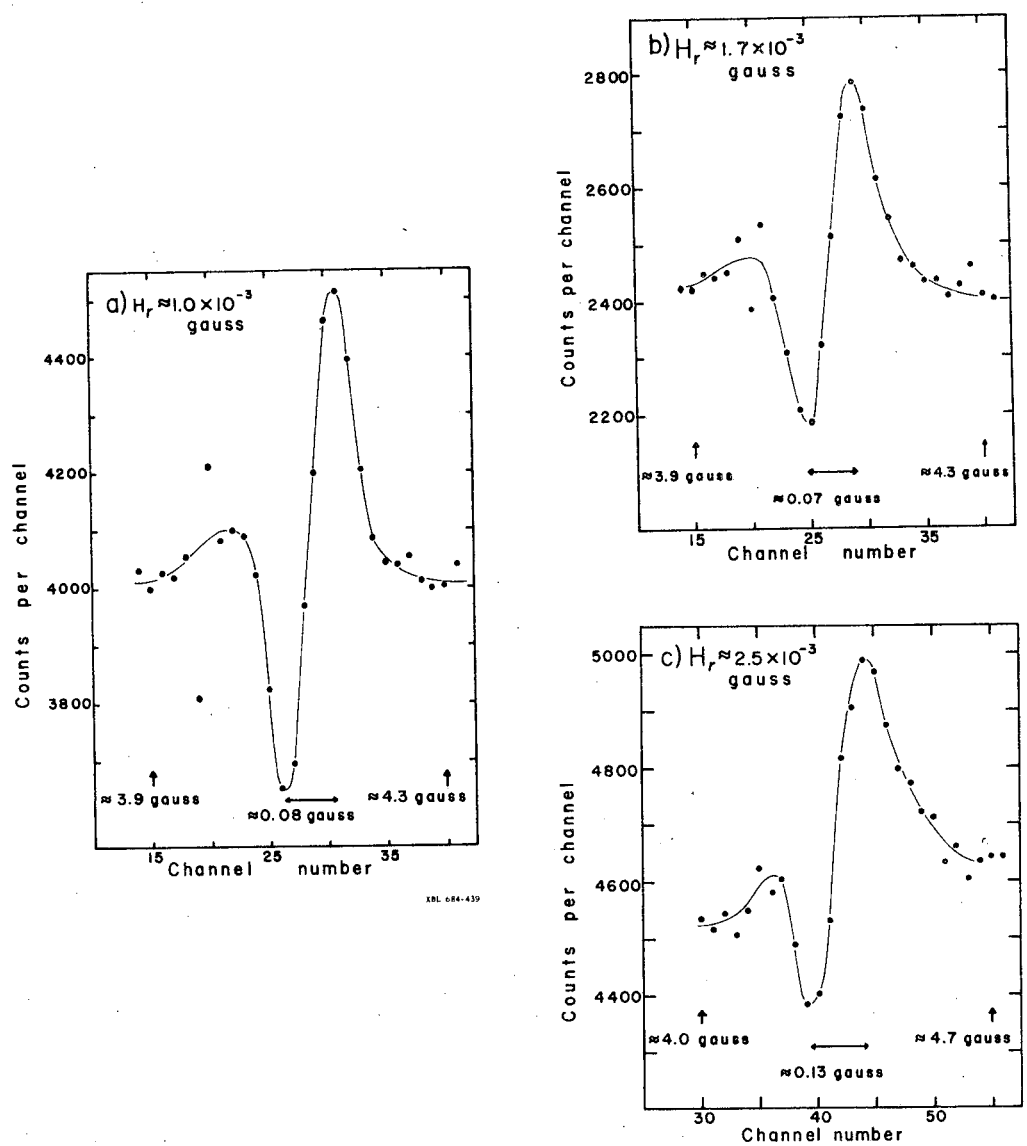

XBL 684-708

Fig. 6. An example of the effectiveness of taking measurements only when the electron gun's heater current is not flowing. The line width should increase steadily with rf power. Figure (b) was, however, taken during the half cycles when the pulsed heater current was off, while (a) and (c) were obtained with the current constantly on. The lines in (a) and (c) have apparently been broadened by the magnetic field set up by the heater current.

$$A \propto \frac{1}{(G+2g)^2+(\gamma H_r)^2+(\omega-\omega_0)^2} \quad ,$$

$$\frac{dA}{d\omega} \propto -2(\omega-\omega_0)[(G+2g)^2+(\gamma H_r)^2+(\omega-\omega_0)^2]^{-2}$$

$$\frac{d^2A}{d\omega^2} \propto 8(\omega-\omega_0)^2[(G+2g)^2+(\gamma H_r)^2+(\omega-\omega_0)^2]^{-3} \; -2[(G+2g)^2+(\gamma H_r)^2+(\omega-\omega_0)^2]^{-2} \quad ,$$

and therefore

$$(\omega_{\text{inflection}}-\omega_0) = \frac{1}{\sqrt{3}}[(G+2g)^2+(\gamma H_r)^2]^{\frac{1}{2}} \quad .$$

The comparable expression for the half width gives

$$\tfrac{1}{2}\left[\frac{1}{(G+2g)^2+(\gamma H_r)^2}\right] = \frac{1}{(G+2g)^2+(\gamma H_r)^2+(\omega_{\frac{1}{2}}-\omega_0)^2} \quad ; \text{ or}$$

$$(\omega_{\frac{1}{2}}-\omega_0) = [(G+2g)^2+(\gamma H_r)^2]^{\frac{1}{2}} \quad , \text{ and}$$

$$(\omega_{\text{inflection}}-\omega_0) = \frac{1}{\sqrt{3}}(\omega_{\frac{1}{2}}-\omega_0) \quad .$$

One would expect, then, that the distance between the peaks in the first-derivative curve would give a measure of the line width in the more general case also. In Fig. 6 the three line widths should increase steadily with r-f amplitude, but the middle curve, which was taken when the heater current was pulsed, is clearly narrower than the series taken with the heater on all the time. We continued, therefore, to use the pulser and gating system.

B. Lamp

The lamps providing the resonance light that monitored the atomic alignment were electrodeless discharge tubes filled with the appropriate

(mercury or neon) gas. The first few lamps used were discharged at a radio frequency with power up to 500 watts. To obtain maximum voltage across the lamp, the line from the power supply was tunable, and the coil around the lamp was part of a resonant parallel LC circuit. These lamps were not unsatisfactory but were somewhat clumsy and quite sensitive to tuning. The later lamps were discharged in a microwave cavity powered by a 2.54 kMc Burdick MW200 microwave unit; this produced as bright a light, and also was more compact and much more stable. The lamps were made of quartz, since they became very hot in use. They were baked out under vacuum and filled in a manner similar to filling the electron guns. Further outgassing of the neon lamps was accomplished by discharging the neon while the lamp was still connected to the vacuum system, then pumping out and re-filling. The optimum pressures, i.e., the pressures which produced the strongest neon 6143Å or mercury 5461Å line, were determined by trial and error, by discharging the lamps under conditions which were the same as in the actual experiment and comparing the responses of the photomultiplier tube; the best results were obtained with 3-5 Torr, measured at room temperature. The light leaving the lamp was collimated into a beam of about the same cross section as that of the interaction region (between cathode and anode) in the gun and was polarized in the z direction before entering the gun.

C. Vacuum System

The vacuum system was especially designed so that the lamps and electron guns made on it could be baked out. An electrically heated

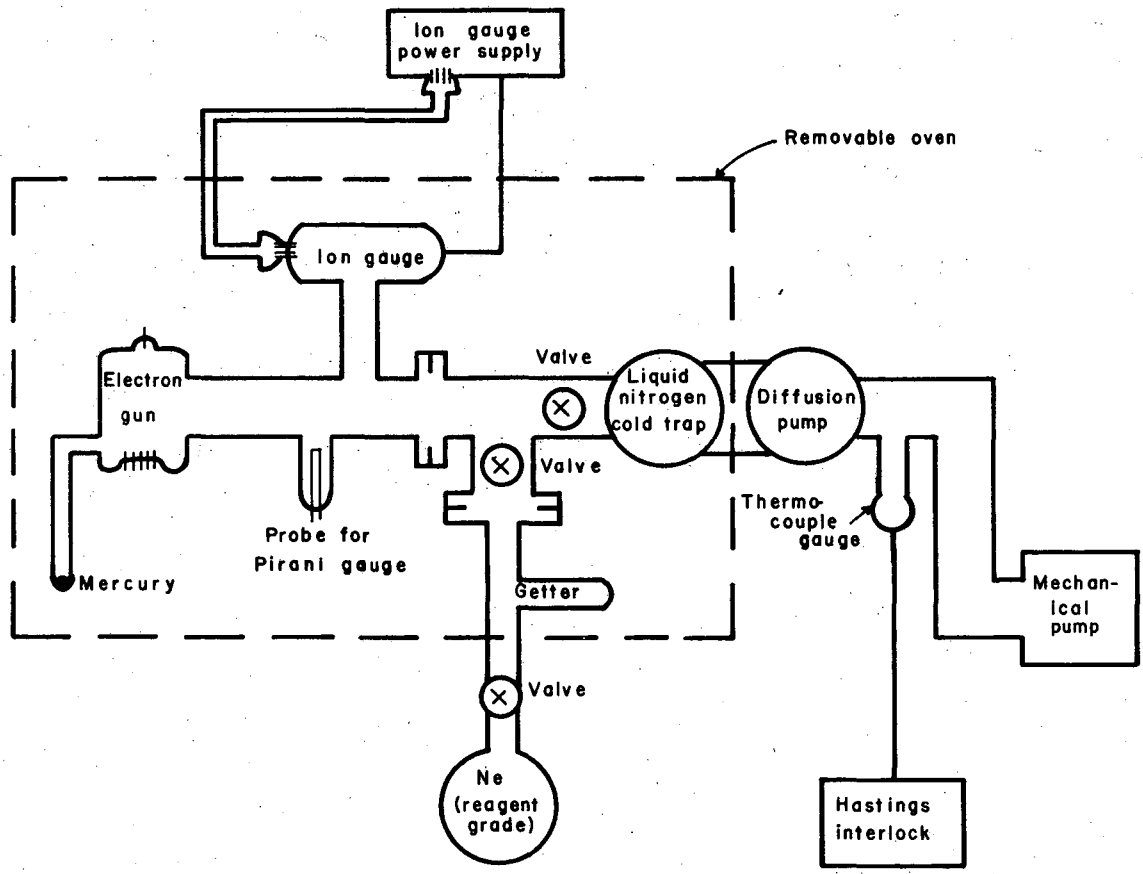

XBL 684-441

Fig. 7. A block diagram of the vacuum system.

oven could be lowered down over the liquid nitrogen trap, ionization gauge (and Pirani gauge, when included) and apparatus under construction. Among other things, this meant that the valves in that part of the system had to be bakeable. At first we used converted, non-bakeable Vecco valves in which the teflon gaskets were replaced with indium. Indium melts at 155° C and is soft at room temperature, so it is not only easy to seat the valve firmly, but also the indium should form a new, smooth surface with every bakeout. In spite of all precautions, however, the molten indium did not always wet the valve body around the entire circumference of the gasket, which usually prevented a complete seal. We turned, therefore, to commercially-produced bakeable valves, and a new vacuum system was designed using Varian valves with replaceable copper alloy gaskets. At the same time, the mechanical pump backing up the oil diffusion pump was moved outdoors to eliminate any danger of mercury vapor being pumped into the room. Otherwise, the pump-out lines were kept as short and as broad as possible. As mentioned above, it was not difficult to obtain pressures of 10^{-8} Torr after a few hours of bakeout. A thermocouple gauge monitored the pressure between the mechanical pump and the diffusion pump and was connected to a Hastings interlock system to shut down the diffusion pump should its forepressure rise too high. An ionization gauge measured the pressure at the lamp or electron gun before and after bakeout and during activation of the guns. A Pirani (thermal conductivity) gauge was used to measure the pressure of the mercury or neon in the lamps and in the neon-filled guns.

D. Steady-State and Radio-Frequency Magnetic Fields

A pair of Helmholtz coils 18 in. in diameter provided the constant field in the z direction; the field throughout the interaction region in the electron gun should have been uniform to one part in 10^4. Since we generally worked at fields of 2 to 7 gauss, the earth's magnetic field would have contributed a major distortion; for this reason, the horizontal component of the field due to the earth was cancelled with a pair of 26 in. coils (the vertical component was included in H_z, since the z axis was in that direction).

Actually H_z was not strictly constant. In order to trace out the resonance line, the magnitude of the field was very slowly increased and decreased through the point at which the resonance should take place, given the particular value of the radio frequency employed at the time. This slow field sweep became the x axis on the pulse height analyzer, where the resonance was eventually displayed, and in order to make the movement more uniform than would be possible by hand, it was done either mechanically, by a motor turning up a Variac that controlled the line voltage to the field power supply, or by electronically varying the power supply output. The latter method was the most satisfactory, partly because the sweep was smoother, and partly because the repetition rate was more easily controlled. In the system's final form, an Exact Function Generator, Type 250, controlled the output of a Trygon Electronics, Inc., power supply, with the result that the current through the Helmholtz coils and a series resistor followed the form of the chosen function. The voltage

for the channel advance in the pulse height analyzer was taken from across the series resistor so that the analyzer pictured exactly the appled field.

The radio-frequency was provided by a pair of 2.6 in. loops at right angles to the Helmholtz coils, one loop on either side of the electron gun. Our biggest concern was to be able, on the one hand, to put in enough rf power to cause a resonance without, on the other hand, discharging the vapor in the gun. The two loops were constructed as part of a resonant series LC circuit, in which the capacitor could be changed with the frequency. They were made of very heavy wire and were connected in parallel. With this arrangement, we were able even to chop the rf current on and off without discharging the vapor in the gun.

The magnitude of the rf field was not, as explained in Section II. E., measured exactly. Relative values were obtained by measuring the voltage drop across a 0.9 ohm resistor connected into the circuit just before the rf loops. As mentioned above, this did not yield the true value of the current since, as closely as could be measured with the standard equipment available, the true impedance of the "resistor" at 8 Mc/sec was 15-18 ohm. A standard rf current meter could not be used, as the magnet in it distorted H_z enormously. For the sake of finding the appropriate region in which to work, however, the approximate field could be calculated from the apparent current and the known geometry. As is obvious either from the uncertainty principle or from

the equation for the resonance line, H_r has to be of the order of $1/\gamma\tau = \hbar/\mu_0 g_J \tau$ for an appreciable resonance to take place.

E. Detection System

The monitoring light, having passed through the electron gun, was picked up by a photomultiplier tube preceeded by the appropriate (6143Å or 5461Å) interference filter. In addition to the mumetel shield around the photomultiplier tube, an 18 in. lucite light pipe was cemented to its face in order that the tube itself need not be inside the Helmholtz coils, where the magnetic field could have been strong enough to interfere with its operation. For the g_J measurements an RCA 7102 tube was used; for the mercury lifetime measurements we used an EMI 9558 tube. Both were wired to measure current, as the incident light was quite strong, the portion absorbed in the electron gun being at most only about 20 percent of the total resonance light emitted by the lamp. For the lifetime measurement, the output of the photomultiplier tube was, as mentioned above, gated to be different from zero only in those intervals during which the gun's cathode heater was off.

The basic procedure for detecting the resonance was to choose a radio frequency; set H_z to increase slowly from a low field, through the point $H_z = \hbar\omega/\mu_0 g_J$, to a higher field; and watch the photomultiplier output increase (or decrease) slowly from zero, to a maximum (or a minimum), and return to zero again. So as to increase the signal-to-noise ratio, however, the resonance was made into an a.c. signal to which a lock-in amplifier could respond. The first method we used was to superimpose on H_z a small oscillating field in the z direction

and to take this modulation frequency as the reference frequency for the lock-in amplifier. The result, as has been seen in Fig. 6, is a curve which is the derivative of the normal line shape. A second way to modulate the signal is to turn the rf field on and off very rapidly. At first we hesitated to do this for fear of discharging the gas in the electron gun, but as it turned out, the rf system worked so well that we were able without any trouble to chop the current to the rf loops with a square wave. The advantage of this method is that one then obtains (see, for example, Fig. 12) the normal line shape. Modulation frequencies of up to 1000 cps were used in each case. The rate at which the "constant" magnetic field was changed depended on the range of the sweep and on the integration time of the lock-in amplifier. In general, the pertinent variables were adjusted such that at least three integrations periods were spent in each channel of the pulse height analyzer.

The pulse height analyzer was added to the detection system because the signal-to-noise ratio of the neon resonance was very small even with the use of the lock-in amplifier. (Even with the analyzer it was usually necessary to count for about 2 hours in order to observe a clean neon resonance.) To make a proper input for the pulse height analyzer, the output of the lock-in amplifier was sent through a Dymec Voltage-to-Frequency Converter (after first, however, blocking off with a battery most of the lock-in amplifier's d.c. output); thus strength of signal was made proportional to number of pulses per time. As was mentioned above, the H_z Helmholtz coils were in series with a resistor, the voltage

across which was to be proportional to channel number in the analyzer. This field sweep voltage and the signal pulses from the voltage-to-frequency converter were combined by a Lawrence Radiation Laboratory-built "voltage-to-pulse height converter", which made the height of each pulse proportional to that field sweep voltage at which it occurred (see Fig. 2). The analyzer stored number of pulses versus pulse height; therefore, what was actually recorded was the strength of the signal versus the value of H_z. The wave form used to sweep H_z could be either a sawtooth wave, which swept the field both up and down, or a ramp, which swept the field in only one direction. Both were used, depending on the range of the sweep and the integration time of the lock-in amplifier. The advantage of the ramp wave form was, obviously, that for a given frequency of the function generator, the ramp provided a field sweep that was only half as fast as that of the sawtooth wave.

IV. RESULTS AND DISCUSSION

A. Neon g_J

Since the g_J values of both metastable mercury and neon have already been determined to far greater precision than we had in these measurements [$(g_J)_{Hg} = 1.5099(10)$[21] and $(g_J)_{Ne} = 1.500888(5)$[22]], the point here is not to provide new numbers for the g_J's, but to demonstrate the ability of this method to measure excited-state fine structures or hyperfine structures in the heavier noble gases, to which this method had not previously been applied. In this respect the results are good. The neon resonance shows the expected opposite sign from that of the mercury resonance, thus bearing out the explanation for the resonance (see Figs. 8 and 9; what is not clear from just looking at these curves, however, is that both have knowingly been inverted by the particular adjustment of the d.c. input to the voltage-to-frequency converter--see below--so that although in this example their absolute signs appear to be wrong, the signs are, in fact, as given by the explanation). The field at which this resonance takes place can be determined, with respect to the mercury resonance, fairly accurately. For a sample calculation of $(g_J)_{Ne}/(g_J)_{Hg}$ see the three curves in Figs. 8, 9, and 10. The mercury resonance is used to calibrate the pulse height analyzer; we find that the resonance at 6.596 Mc/sec takes place at channel number 96¼, and the resonance at 7.000 Mc/sec occurs at channel number 107¼. The neon resonance takes place at channel number 106. The ratio of the two g_J values is, for identical frequencies, in the inverse proportion to the two fields at which the resonances occur, and the scale of the magnetic field is directly proportional to the ratio of frequency per channel as

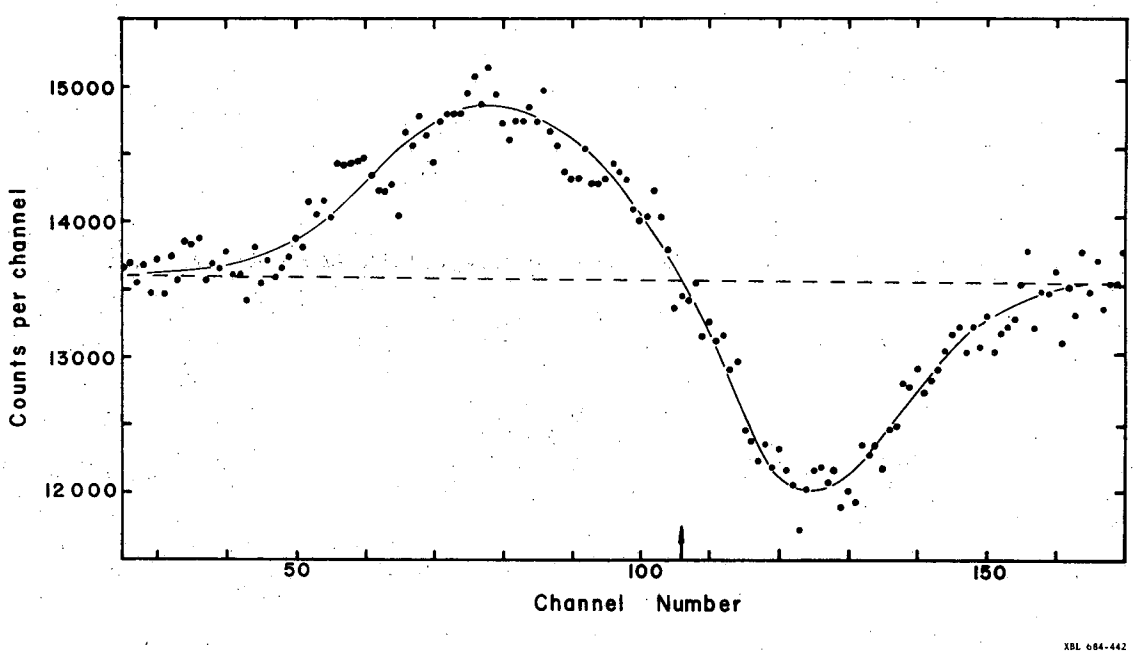

Fig. 8. A neon resonance at 7.000 Mc/sec.

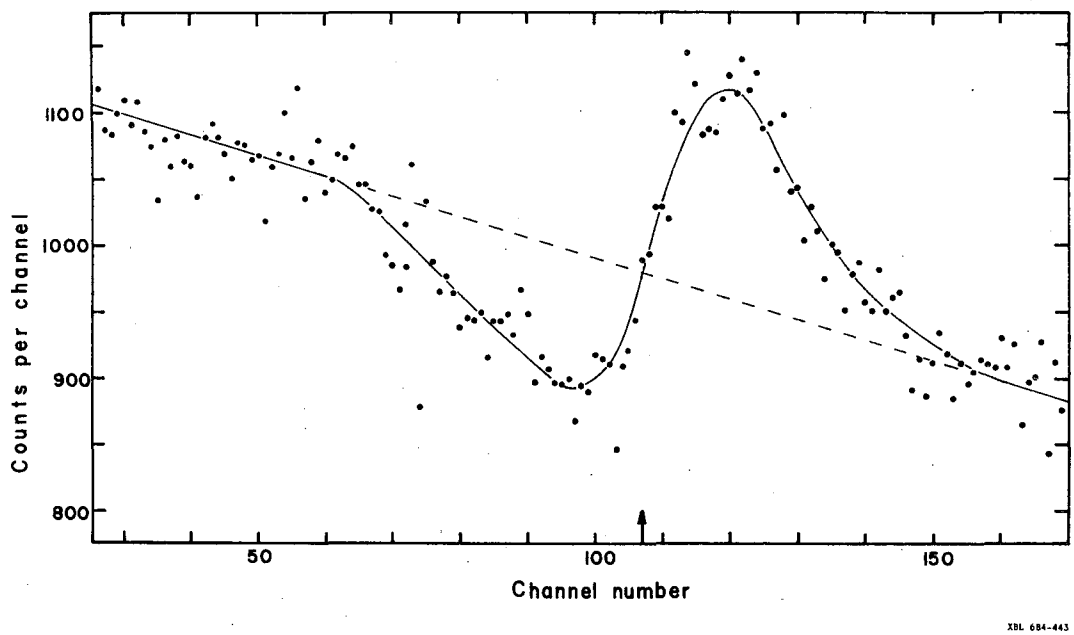

Fig. 9. A mercury resonance at 7.000 Mc/sec.

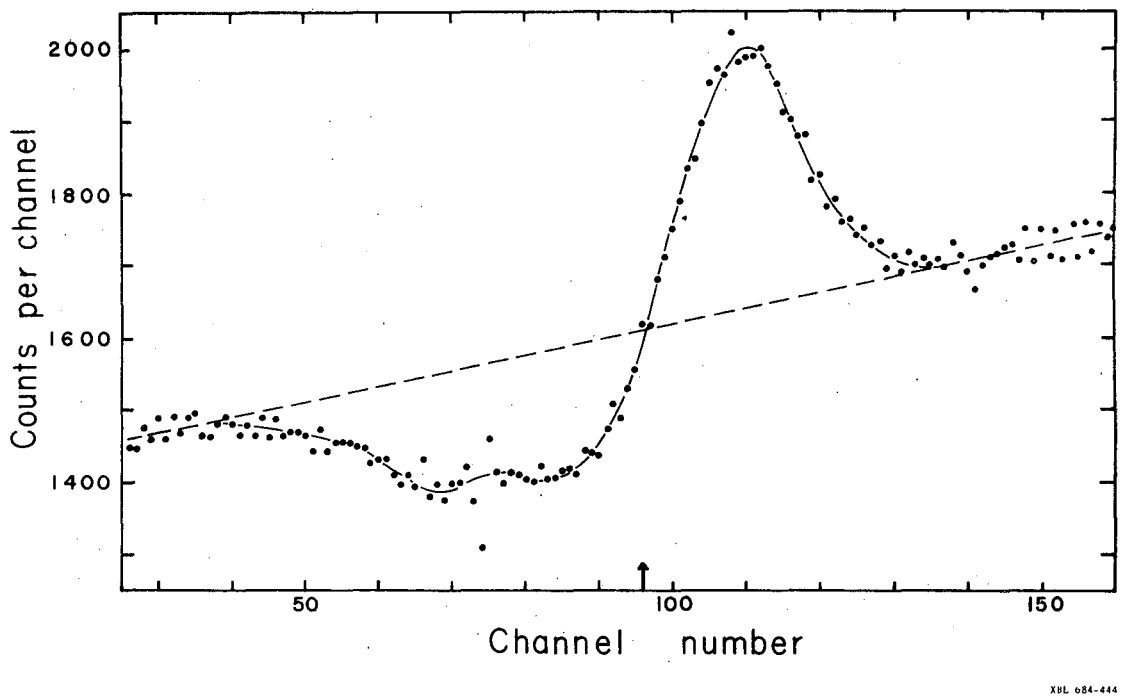

Fig. 10. A mercury resonance at 6.596 Mc/sec.

given by the mercury resonances. Thus we have

$$\frac{(g_J)_{Ne}}{(g_J)_{Hg}} = \frac{(H_0)_{Hg}}{(H_0)_{Ne}} = \frac{7.000\text{Mc/sec}}{7.000\text{Mc/sec} - (1.25\text{ch.})(.404\text{Mc/sec/11ch.})} = 1.006 \ .$$

The error involved in choosing the exact channel in which a given resonance took place is probably not as great as ±2 channels. The biggest problem, as can be seen from the experimental curves, is in determining the position of the base line which these first-derivative curves cross at their midpoint. Figure 10 is an example in which the base line has been disguised even further by the particular operation of the voltage-to-frequency converter. As mentioned in section III. E. the rather large (8V) d.c. output of the lock-in-amplifier was partially blocked off with a battery; otherwise the genuine signal would have been only an extremely small part of the input to the voltage-to-frequency converter. On the other hand, it could not be entirely blocked off since the voltage-to-frequency converter does not, in the frequencies it puts out, distinguish between a positive and a negative input, and the resonance curve of course goes both positive and negative. Thus the trick is to adjust the battery-offset so that the d.c. level is almost zero but far enough from it that the resonance does not cause it to change polarities. Figure 11 shows a series of slightly rf-saturated cesium resonances for which the d.c. level was initially almost zero and was progressively increased; that half of the curve which should be negative is seen to drop down gradually and approach the expected "dispersion" curve shape. Comparison of figures 10 and 11 explain why the former looks so odd: the battery-offset was poorly adjusted. With this in mind,

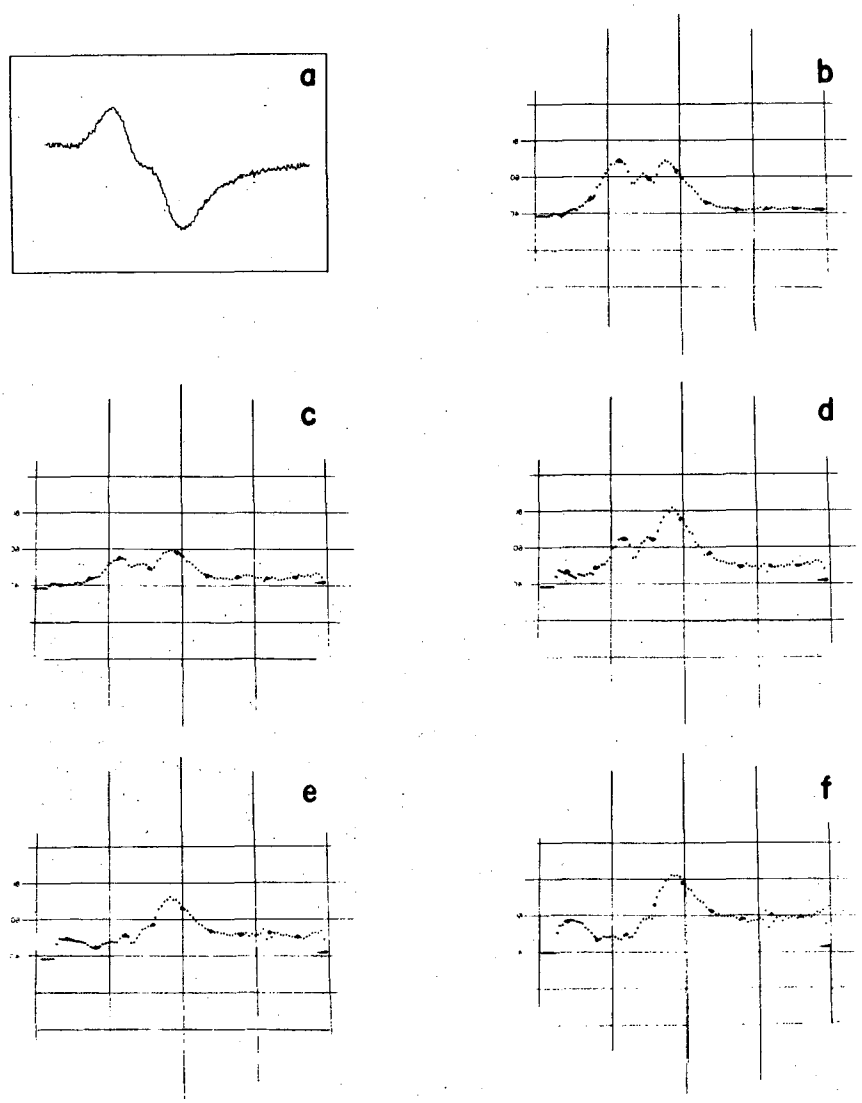

XBL 684-709

Fig. 11. A series of resonances showing the effect of changing the d.c. input to the voltage-to-frequency converter. Figure (a) is a mercury resonance included because it is a very clear-cut example of the shape of the derivative of an rf-saturated line. Figure (b) is a cesium resonance which should have very much the same shape. The d.c. level in (b) was, however, almost zero, and the voltage-to-frequency converter reflected the negative half of the signal through the zero voltage line. In Figs. (c) through (f) the d.c. level of the cesium signal was progressively increased, and one can see the resonance line gradually taking on its expected shape.

the base line in Fig. 10 was drawn simply as if the lower part of the resonance were entirely displayed. Even with this kind of uncertainty, however, the various possible positions of the line do not change by much the number of the channel in which the crossing apparently takes place, for the reason that the resonance curve is steep enough at this crucial point that a relatively large vertical displacement of the base line corresponds to only a small change of the curve in the horizontal direction. Assuming, therefore, that each one of the resonances involved in the $(g_J)_{Ne}/(g_J)_{Hg}$ ratio above can be determined to better than ±2 channels, the error in the ratio implies that for this example $(g_J)_{Ne}/(g_J)_{Hg} = 1.006 \pm .015$. Combining this with other data, we obtain an average value of $1.006 \pm .010$.

It is not difficult to see how this, or a similar measurement, could be made more accurate. For example, after these data were already taken, we found that the expected difficulties in modulating the rf field rather than the H_z field did not materialize: with the normal line shape which results from the former approach it is much easier to determine the exact resonance point, since a peak is more obvious than the position of the base line. See, for example, Fig. 12; here the point of resonance can probably be established to within a channel. In addition, accuracy could be improved by taking measurements at higher fields, where resonances corresponding to different atomic constants would take place at relatively more widely-spaced fields.

Since we have, so far, obtained only the ratio of the metastable-state g_J values (which agrees, as far as it goes, with the more precise measurements already mentioned), it is of interest to calculate at least

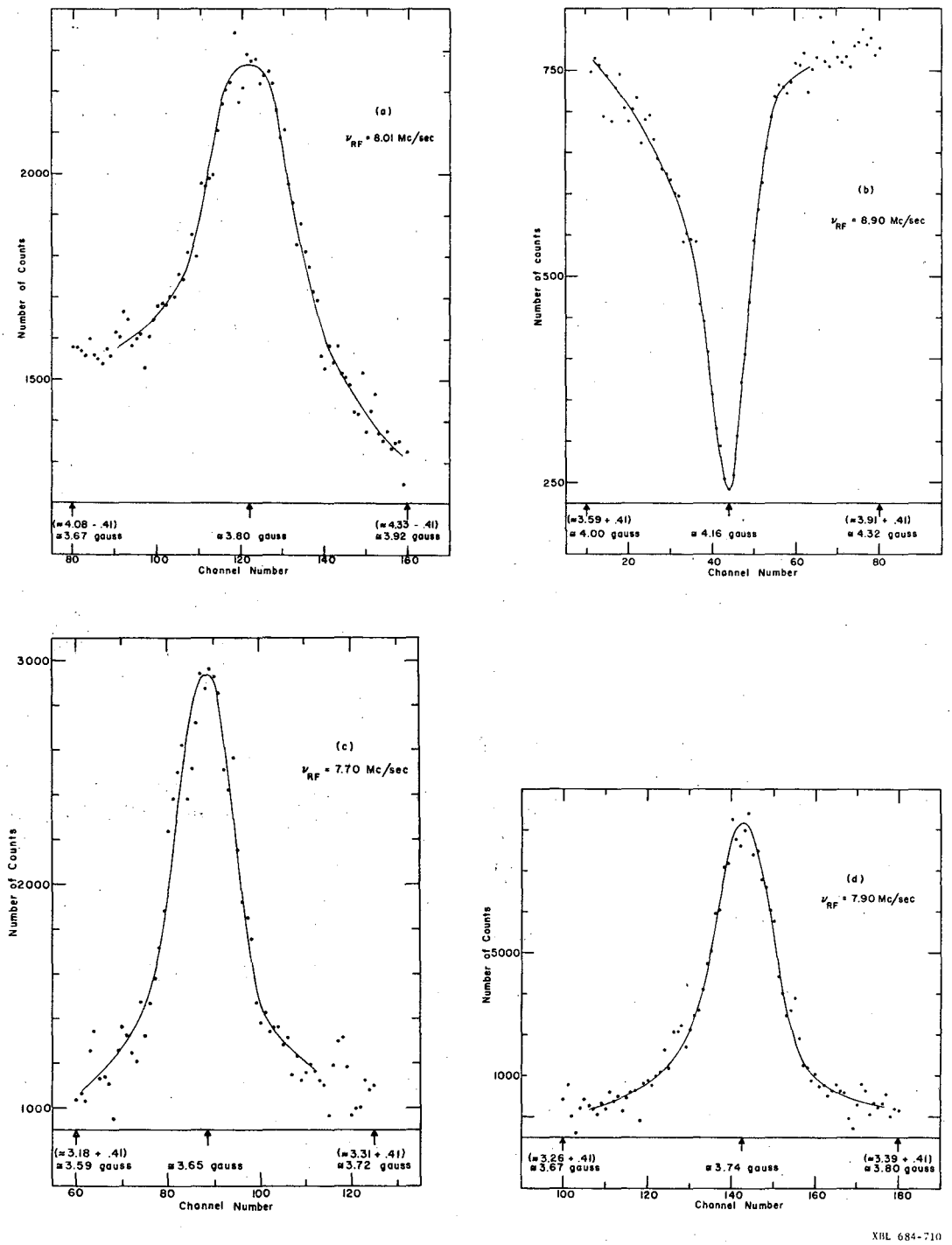

Fig. 12. A sampling of mercury resonance lines used to verify that the mercury resonance takes place at approximately the expected field.

one of the g_J's directly from experimental quantities as a check to make certain that the numerical values are what one would expect. The major source of error will be in the value of the magnetic field at resonance. In general, the current into the Helmholtz coils was noted at the two end points of its sweep and the field at those two points calculated from the known geometry of the coils, with the earth's field being either added or subtracted, depending on the orientation of the coils. This is, however, more indirect than one would normally like, and the value of the magnetic field inside the plasma is also uncertain.

Figure 12 (a), (b), (c), (d), shows four mercury resonances, chosen because they were taken on different days and thus should provide a wider sampling. For the first one, the magnetic field due to the earth was in the opposite direction from H_z, and 0.41 gauss, the value of the earth's field measured by a gaussmeter with the electron gun removed, was subtracted from the applied field; for the other three, H_z and the earth's field were in the same direction. The value of the field at resonance was determined from the position of the peak along the x axis. The apparent g_J values calculated from these four resonances are

Fig. 12	Date Taken	ν_{rf}	$H_0=H_z$ at resonance	g_J
Fig. (a)	06-23-65	8.01 Mc/sec	3.80 gauss	1.50
Fig. (b)	07-28-65	8.90 Mc/sec	4.16 gauss	1.53
Fig. (c)	08-11-65	7.70 Mc/sec	3.65 gauss	1.51
Fig. (d)	09-23-65	7.90 Mc/sec	3.74 gauss	1.51

These rough numbers for the mercury gyromagnetic ratio are close enough to the more precise value to assure us that the experimental set-up is working correctly and that the mercury resonance, taken as a known parameter, could be used to give the numerical value of the neon metastable-state g_J. Thus it can be concluded that this method is suitable for determining unknown fine structures (and, presumably, hyperfine structures) in the excited states of the noble gases.

B. Mercury Lifetime

The process of measuring the lifetime of the metastable mercury m-state passed through several stages. The initial efforts involved numerically integrating the experimental first-derivative curves to obtain the normal line shape, so as to be able to measure directly the half-widths of the lines. As described in Section IIE, the lifetime can be obtained by plotting the square of the half width, $\Delta\omega$, against the square of the rf power for gradually decreasing rf power, and by then extrapolating what should be a straight line to zero rf field, at which point the half width should be due entirely to the finite lifetime. It would have been convenient if it had been possible to find a similarly simple relationship between the lifetime and the two peaks of the dispersion-shape curve (the two inflection points of the real resonance line). Except in the limit $(\gamma H_r) = 0$, at which point $(G+2g) = \sqrt{3}(\omega_i - \omega_0)$, the relationship turns out to be very complicated, however, involving powers of $(\omega_i - \omega_0)$ up to $(\omega_i - \omega_0)^8$. Thus, unless one were able to measure H_r exactly, in which case it would be possible to substitute into the equation numerical values for γH_r and $|\omega_i - \omega_0|$ and solve for $(G+2g)$ with

a computer, it appears that measuring the half width is the more practical approach.

An example of an experimental dispersion-shape curve and the normally shaped resonance line obtained from it by numerical integration is given in Figure 13, where it can be seen that this particular procedure is not unreasonable. The integrated line turns out to be slightly asymmetric (as are the experimental lines in, for example, Fig. 12), but as one can see, the half width occurs close enough to the inflection point that it is not made too uncertain by this. A rough value for the combined lifetimes obtained from a set of curves like this is $(G+2g) = 3.04 \times 10^6\ \mathrm{sec}^{-1}$; see Fig. 14. This value is called "rough" because it is clear that it is not correct. This run was made while the electron gun was still attached to the vacuum system, and in order that the side arm containing the liquid mercury should control the mercury vapor pressure, an attempt was made to heat with heating tape the stainless steel and glassware of the vacuum system between the gun and the valve to the cold trap and diffusion pump. Apparently the heating tape produced a relatively large magnetic field, however. A set of resonances recorded at various vapor pressures shows no discernible change of the line width with pressure, implying that the atomic lifetime was not the controlling factor, since it should be dependent on the collision rate. (The rf power was not at fault; the resonances did not begin to show rf saturation until a relative field amplitude of 6, so the rf powers used in general would be considered "small".) Thus if we take it that these resonances are considerably broadened by an inhomogeneous magnetic

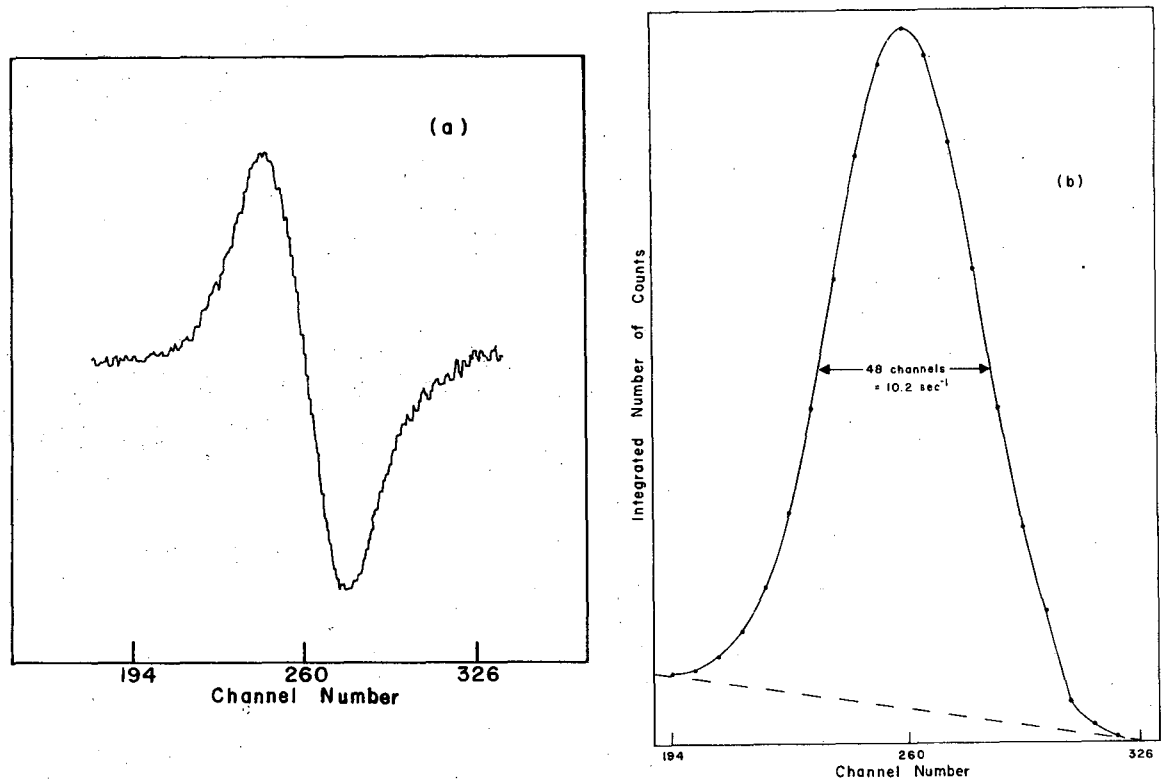

XBL 684-711

Fig. 13. An example of an experimental dispersion-shape curve and the normal resonance line obtained from it by numerical integration. Figure (a) is a recorder trace. The relative rf power here (see Fig. 14) is 2.

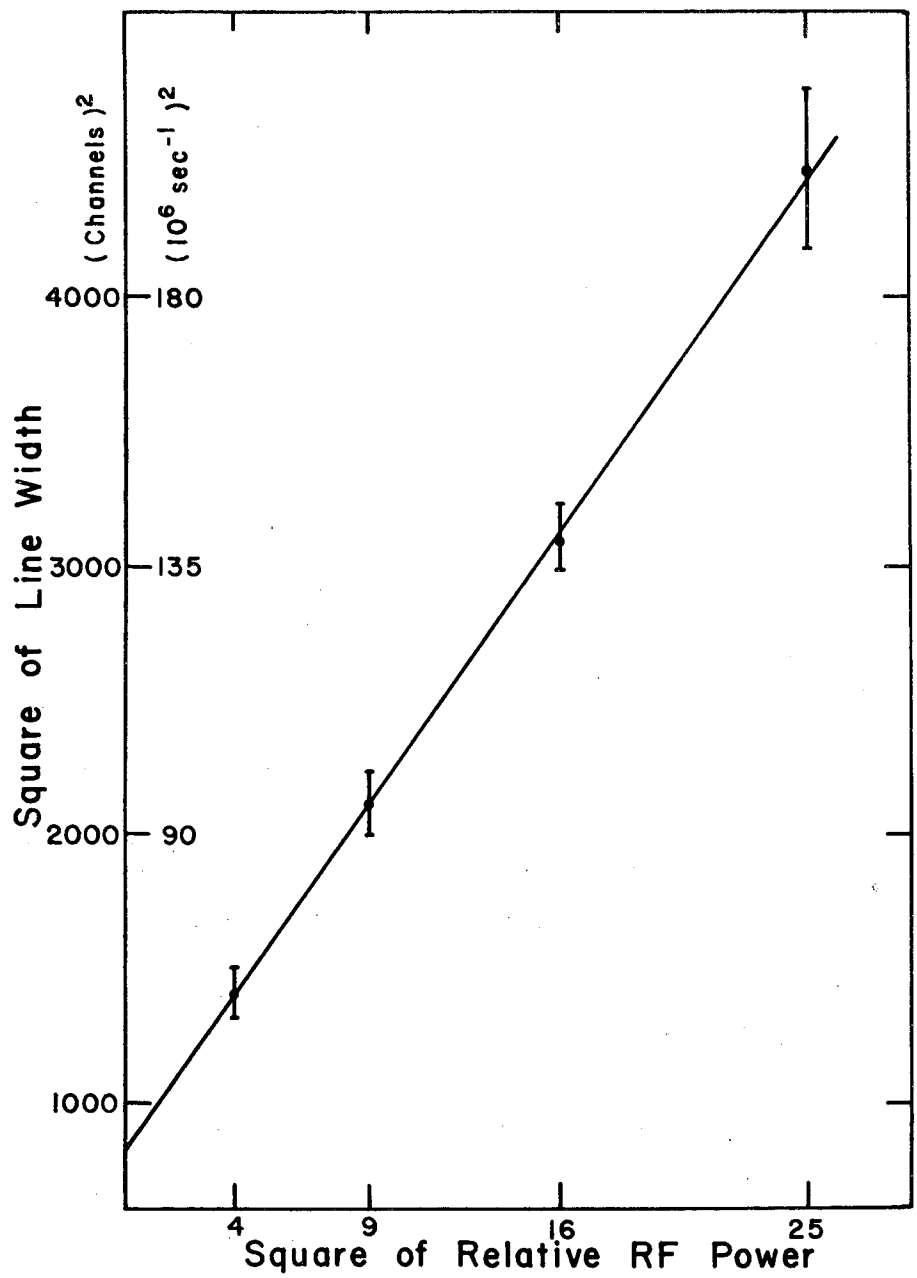

XBL 684-451

Fig. 14. The graph from which is obtained an upper limit for (G+2g) of 3.04×10^6 sec^{-1}. Notice that the square of the full line width has been plotted here, whereas (G+2g) corresponds to $|\omega-\omega_0|$, or half the line width.

field, we know that the m-state lifetime is longer than $\tau_m = 1/g = 0.66 \times 10^{-6}$ sec. (Baumann measured 1/G to be 1×10^{-4} sec to 4.5×10^{-4} sec for similar pressures; it is therefore negligible here.)

The process of numerically integrating the dispersion-shape curves, while not impossible, was rather tedious, and as has been mentioned, it turned out that obtaining the normally-shaped resonance lines directly was not as difficult as expected. Thus when it came to improving upon the above measurements, the resonance signal was obtained by modulating the rf field rather than H_z, with results like those shown in Fig. 12. Unfortunately this run did not last long enough (electronics trouble interrupted it) for us to get good statistics, and so in order to arrive at a new estimate of the m-state lifetime, it was necessary to average together data taken at different pressures. That is, a few measurements had been made at each of the vapor pressures corresponding to temperatures of 21.2°, 25.2°, 28.2°, 31.2°, 35.2°, and 42.2°, and these sets of measurements were combined in pairs, 21.2° and 25.2°, 28.2° and 31.2°, and 35.2° and 42.2°, to produce the graphs of Fig. 15, where the squares of the line widths are plotted against the squares of the rf powers. From the residual line widths at the extrapolations to zero rf field, we find $(G+2g) = (15.3 \pm 1.8) \times 10^4$ sec^{-1}, $(16.9 \pm 3.0) \times 10^4$ sec^{-1}, and $(19.9 \pm 2.8) \times 10^4$ sec^{-1}, respectively. Here G is almost significant, but it still will not affect the values of the lifetime by more than the experimental error. For these three cases, then, $\tau = (1.31 \pm 0.22) \times 10^{-5}$ sec, $(1.19 \pm 0.30) \times 10^{-5}$ sec, and $(1.01 \pm 0.20) \times 10^{-5}$ sec. (Note that τ is, as expected, considerably longer than our first rough estimate.)

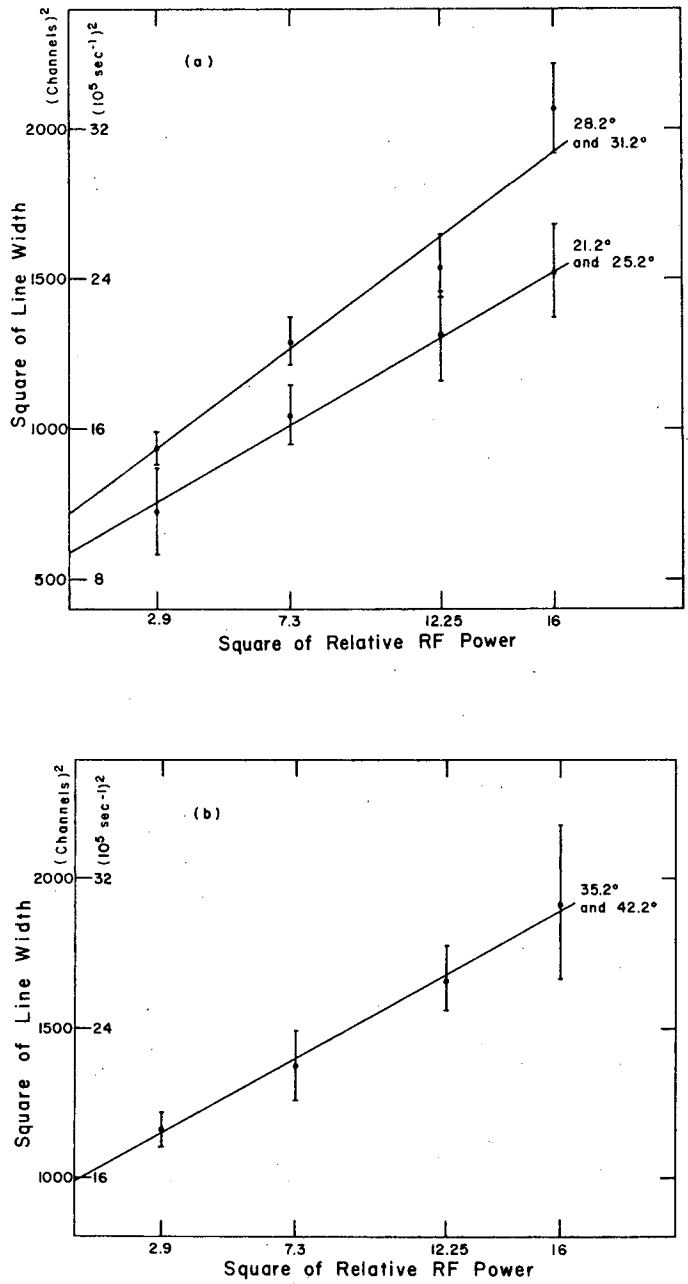

XBL 684-452

Fig. 15. The graphs from which are obtained values of $(G+2g) = 15.3 \times 10^4\ sec^{-1}$, $16.9 \times 10^4\ sec^{-1}$, and $19.9 \times 10^4 sec^{-1}$, in the order of increasing temperature. These data come from mercury resonances observed with a modulated H_r rather than a modulated H_z.

It is of interest to look at these values as a function of pressure. The metastable atoms must be disaligned chiefly by collisions with other atoms in the electron gun[2,3] and the lifetime should be inversely proportional to (or the line width directly proportional to) the density of the disaligning species. One would hope, therefore, that the variation with pressure of the line width would help one to infer the nature of that species and thus also the magnitude of the effective collision cross section. Figure 16 shows that for our three cases the line width increases linearly with pressure; thus so far it looks as if the disaligning atoms are of a kind whose density is proportional to the density of the mercury vapor in the gun. Here the average pressures were arrived at by weighting each of a given pair of pressures by the number of measurements taken there. That is, for 12 measurements made at 21.2° and 12 made at 25.2°, the pressure is plotted half way in between, whereas for 9 measurements made at 28.2° and 4 at 31.2°, the pressure is 9/13 of the way from the respective 2.4×10^{-3} Torr to 3.0×10^{-3} Torr. There were 7 measurements made at 35.2° and 6 at 42.2°. The errors in the residual line widths include both the error involved in determining the intercept of a least squares-fitted straight line[24] and the error in calibrating the pulse height analyzer channel numbers in terms of frequency. The errors in the above values of τ have the same sources.

Since it appeared that quite a few measurements were necessary to obtain meaningful results from this method of graphing and extrapolating to zero rf power, we wondered if there might not be a more efficient way of deducing the m-state lifetime. The procedure that was tried was mentioned in Section II E: The rf power was increased until the broadened

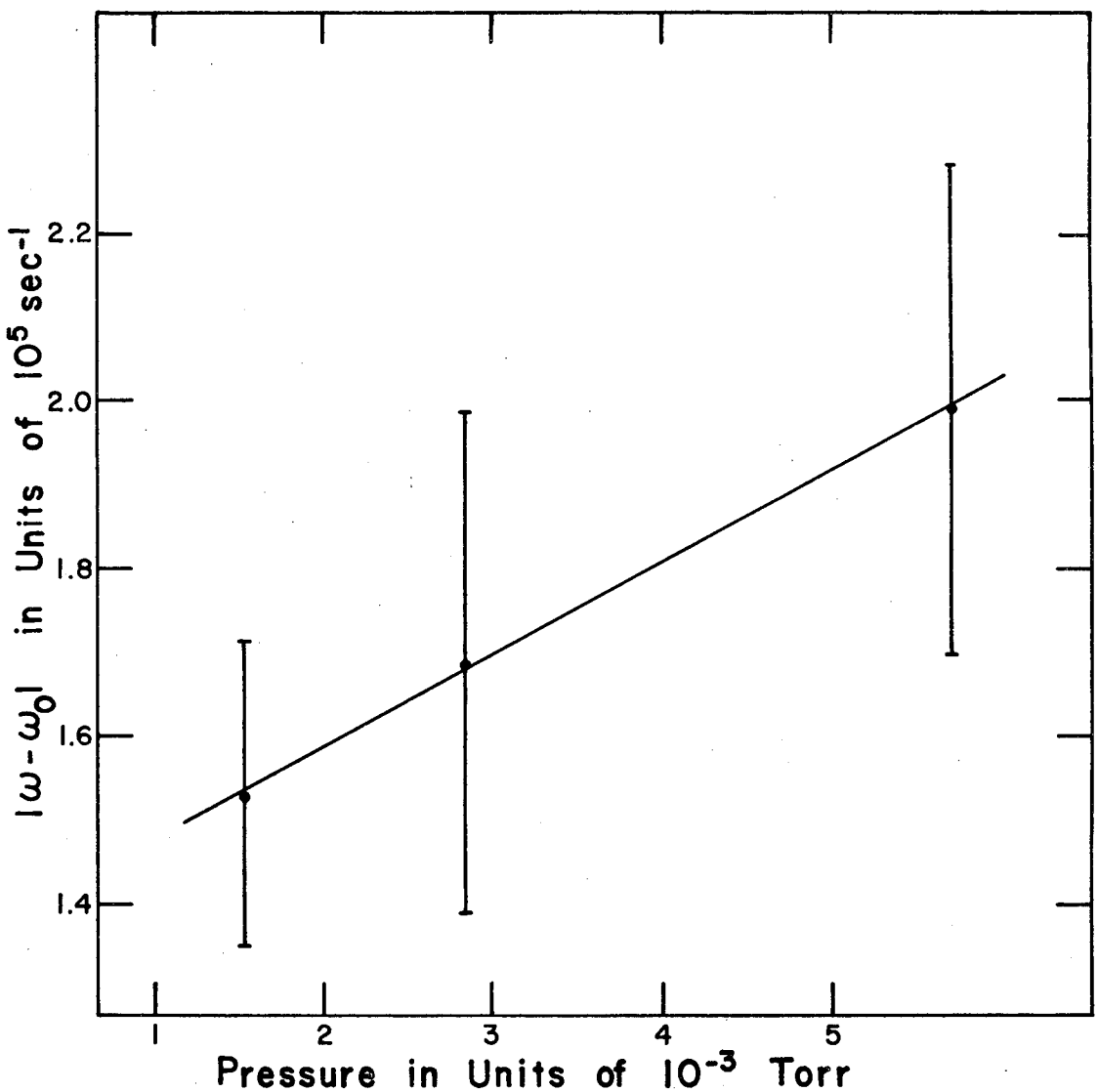

XBL 684-453

Fig. 16. Line width (at zero rf field) as a function of pressure for the normally-shaped resonance lines.

resonance line displayed the characteristic double maxima spaced symmetrically on both sides of the center of the line. From the equation for the line, one can derive the relationship among $|\omega_m-\omega_0|$, (G+2g), and γH_r. Only the relative field strengths are known, but pairs of equations can be combined to obtain

$$\left[\frac{(H_r')_1}{(H_r')_2}\right]^2 = \frac{8(\omega_m-\omega_0)_1^2-7(G+2g)^2+3\sqrt{9(G+2g)^4+64(\omega_m-\omega_0)_1^4+16(G+2g)^2(\omega_m-\omega_0)_1^2}}{8(\omega_m-\omega_0)_2^2-7(G+2g)^2+3\sqrt{9(G+2g)^4+64(\omega_m-\omega_0)_2^4+16(G+2g)^2(\omega_m-\omega_0)_2^2}}$$

where it is assumed that the factor changing relative rf powers into actual field strengths has cancelled out. From this one can solve numerically for (G+2g), using measured values for the $|\omega_m-\omega_0|$ corresponding to each rf power. The advantages of this approach are these: unlike measurements of the line width, the apparent location of the peak is not affected by a poor determination of the base line, or background level; since only the top of the resonance line is of interest it is not even necessary, in fact, to trace out the entire line, which means that the length of time required for each measurement is decreased; and each pair of measurements yields a value for (G+2g) - although this would be true of the line width measurements also, if they were subjected to a similar numerical analysis. In Fig. 17 are some examples of the tops of double-peaked resonance lines. These may be compared with the curves in Fig. 18, where their theoretical counterparts have been plotted from the equation for the line and various ratios of $(G+2g)/(\gamma H_r)$.

Measurements were again made at a number of vapor pressures between those corresponding to 21° and 42°; that is, at 1.3×10^{-3} Torr to

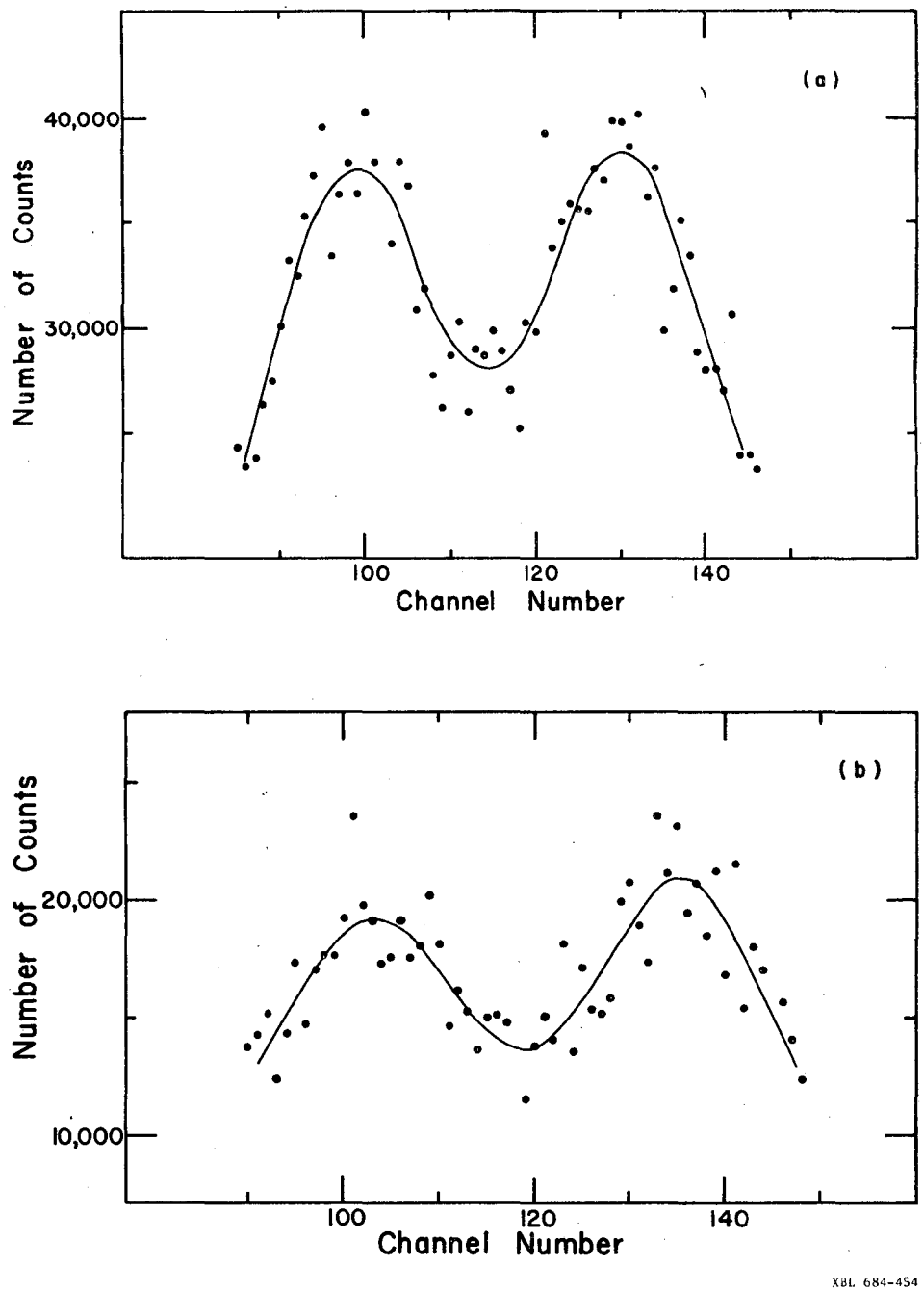

Fig. 17. Two examples of double-peaked resonance lines. Figure (a) was taken at a mercury vapor pressure corresponding to 25.3° C., with a relative H_r of 6.5 volts. Figure (b) was at 21.3° C., with a relative H_r of 7.2 volts.

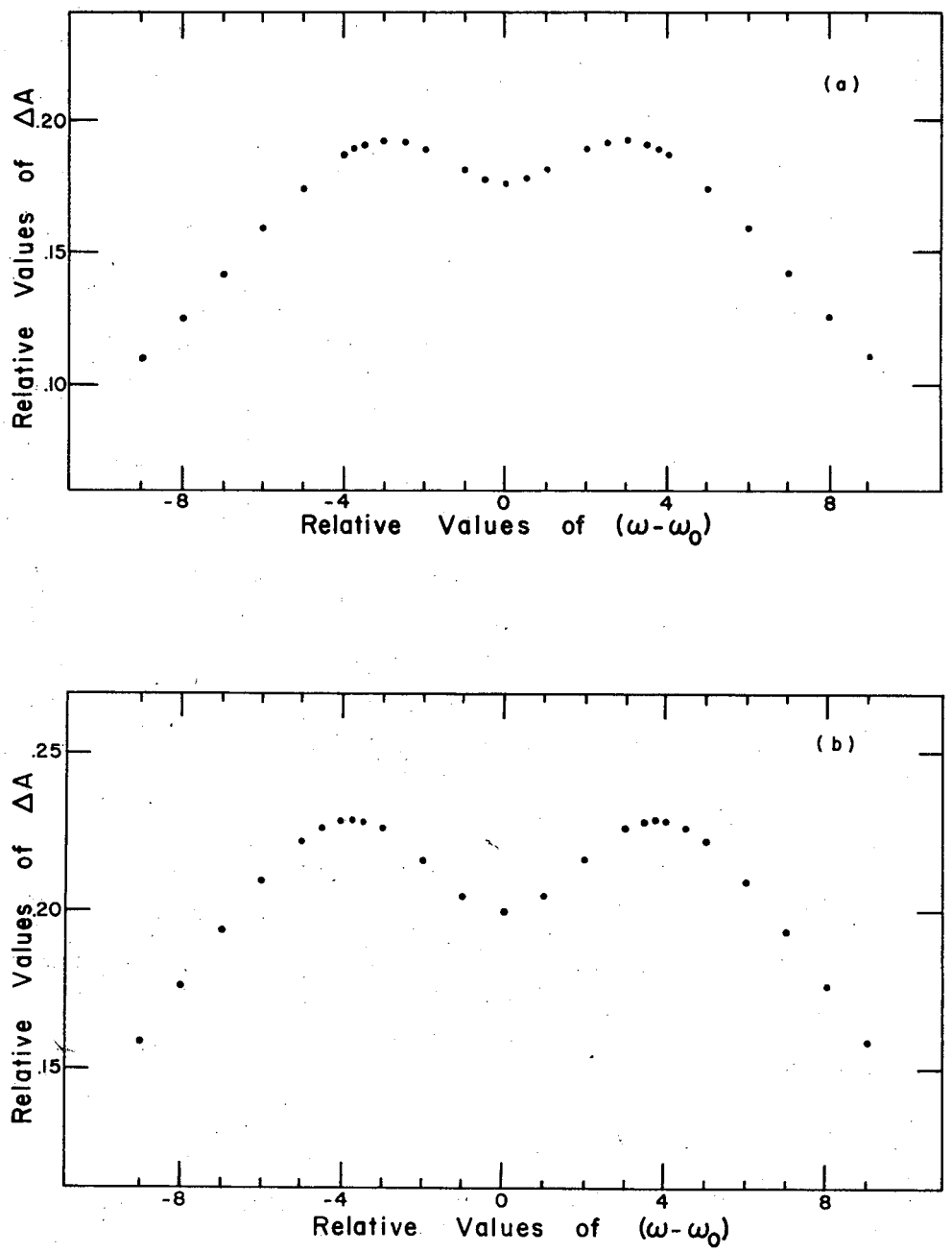

XBL 684-455

Fig. 18. The shape of the double-peaked resonance calculated from the equation for the line. The relative height of the line is

$$\Delta A \propto \frac{(\gamma H_r)^2}{(G+2g)^2+(\gamma H_r)^2+(\omega-\omega_0)^2} - \frac{3(\gamma H_r)^4}{[(G+2g)^2+(\gamma H_r)^2+(\omega-\omega_0)^2][(G+2g)^2+4(\gamma H_r)^2+4(\omega-\omega_0)^2]}$$

for two different ratios of $(G+2g)^2/(\gamma H_r)^2$. In (a) the assumed values are $(G+2g)^2 = 25$, $(\gamma H_r)^2 = 15$; in (b), $(G+2g)^2 = 25$, $(\gamma H_r)^2 = 25$.

7.1×10^{-3} Torr. The rf fields were in the approximate range 16×10^{-3} gauss to 25×10^{-3} gauss and at frequencies of 7.84 and 7.92 Mc/sec. In some cases the resonance seemed to be asymmetric about ω_0; in those instances $|\omega_m-\omega_0|$ was taken to be the average of the two apparent $|\omega_m-\omega_0|$'s.

At first the numerical solutions for (G+2g) were worked out by hand, with a desk calculator, so that it was possible to see what form the solutions were taking. A major difficulty soon became obvious. The expression

$$R(1,2) = \frac{8(\omega_m-\omega_0)_1^2-7(G+2g)^2+3\sqrt{9(G+2g)^4+64(\omega_m-\omega_0)_1^4+16(\omega_m-\omega_0)_1^2(G+2g)^2}}{8(\omega_m-\omega_0)_2^2-7(G+2g)^2+3\sqrt{9(G+2g)^4+64(\omega_m-\omega_0)_2^4+16(\omega_m-\omega_0)_2^2(G+2g)^2}},$$

plotted as a function of (G+2g) has the form shown in Fig. 19. In a number of cases, the measured values of $|\omega_m-\omega_0|$ are such that no value of (G+2g) can make R(1,2) large enough to equal the corresponding $(H_r')_1^2/(H_r')_2^2$. On the other hand, as long as $|\omega_m-\omega_0|_1 > |\omega_m-\omega_0|_2$ whenever $(H_r')_1 > (H_r')_2$, (G+2g) can always be made large enough for R(1,2) to match a relatively small value of $(H_r')_1^2/(H_r')_2^2$. Thus if one were to discard arbitrarily those measurements in which $(H_r')_1^2/(H_r')_2^2$ is larger than R can be but at the same time were to retain those measurements in which this ratio is comparatively small, the resulting average value of (G+2g) would be weighted in favor of the higher experimental values. Another difficulty arises in the few instances in which the measured $|\omega_m-\omega_0|_1 < |\omega_m-\omega_0|_2$ although $(H_r')_1 > (H_r')_2$. In these cases there is again no solution for (G+2g), even though it is impossible to decide that one of the two measurements is "correct" and the other "incorrect". In order to overcome both of these problems, sets of measurements were paired off again, to obtain

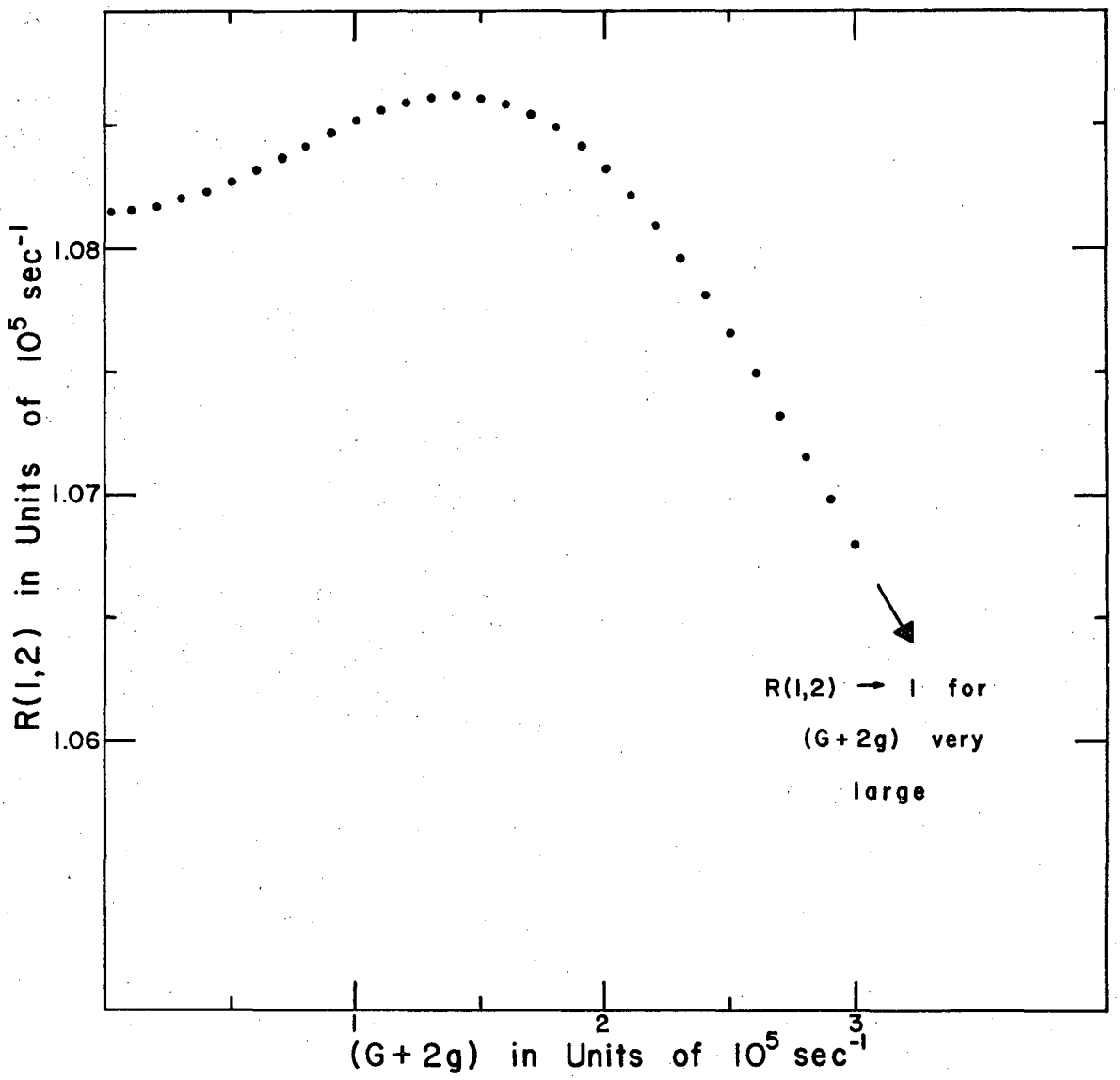

XBL 684-456

Fig. 19. The ratio R(1,2) as a function of (G+2g). This example is for the specific case of two measurements at 35.2° with relative rf powers of 6.8 volts and 5.64 volts and line widths (that is $|\omega_m - \omega_0|$) of 1.47×10^5 sec^{-1} and 1.41×10^5 sec^{-1}. The shape of the curve is the same in general, however.

$$\frac{(H_r')_1^2}{(H_r')_2^2} = \frac{(H_r')_3^2}{(H_r')_4^2} = R(1,2) + R(3,4) \quad ,$$

an equation which should still be true and which should have the effect of averaging line widths which cannot be averaged in a straightforward fashion since they do not correspond to identical values of the rf field. So that each measurement would have an equal weight in the final average, the method that was used to combine them was this: For a given pressure, each $(H_r', |\omega_m - \omega_0|)$ pair was combined with each of the others in the original equation, $(H_r')_1^2/(H_r')_2^2 = R(1,2)$, and then these expressions were just added in pairs, a process wich sometimes worked out evenly and at some pressures meant one of the original equations was left over. When it worked out evenly, the values for (G+2g) were simply averaged; when it did not, the average (G+2g) was obtained by weighting the solution of the "leftover" equation half as much as the solution of the others--it was only necessary that the "leftover" equation be one of those that had a solution.

The final calculations were made with a computer, and the results, (G+2g) at the various pressures, are given in Table I. The same table also gives the lifetimes; these were again calculated with the assumption that G was negligible. The two most outstanding features of these results are: the lifetimes are considerably shorter than those arrived at in the run in which the line width was extrapolated to zero rf field; and (G+2g) is not linear with pressure. Figure 20 shows (G+2g) plotted as a function of pressure; above 31° it increases linearly as in the earlier run, but at low pressures some new effect seems to take over and

Table I. M-state lifetimes obtained from the double-peaked resonances.

Temperature* in degrees C	Pressure[25] in 10^{-3} Torr	(G+2g) in 10^5 sec^{-1}	$\tau = 1/g$ in 10^{-5} sec
21.2	1.3	2.89 ±.11	.69 ±.04
25.2	1.9	2.76 ±.39	.72 ±.14
28.2	2.4	2.46 ±.32	.81 ±.15
31.2	3.1	2.07 ±.44	.97 ±.29
35.2	4.2	2.65 ±.24	.76 ±.10
38.2	5.3	3.09 ±.41	.65 ±.12
42.2	7.2	4.10 ±.28	.49 ±.05

* These temperatures are actually 21.2 ±.2, etc. The resulting uncertainty in the pressure should, however, affect the lifetime only by amounts well within other experimental error.

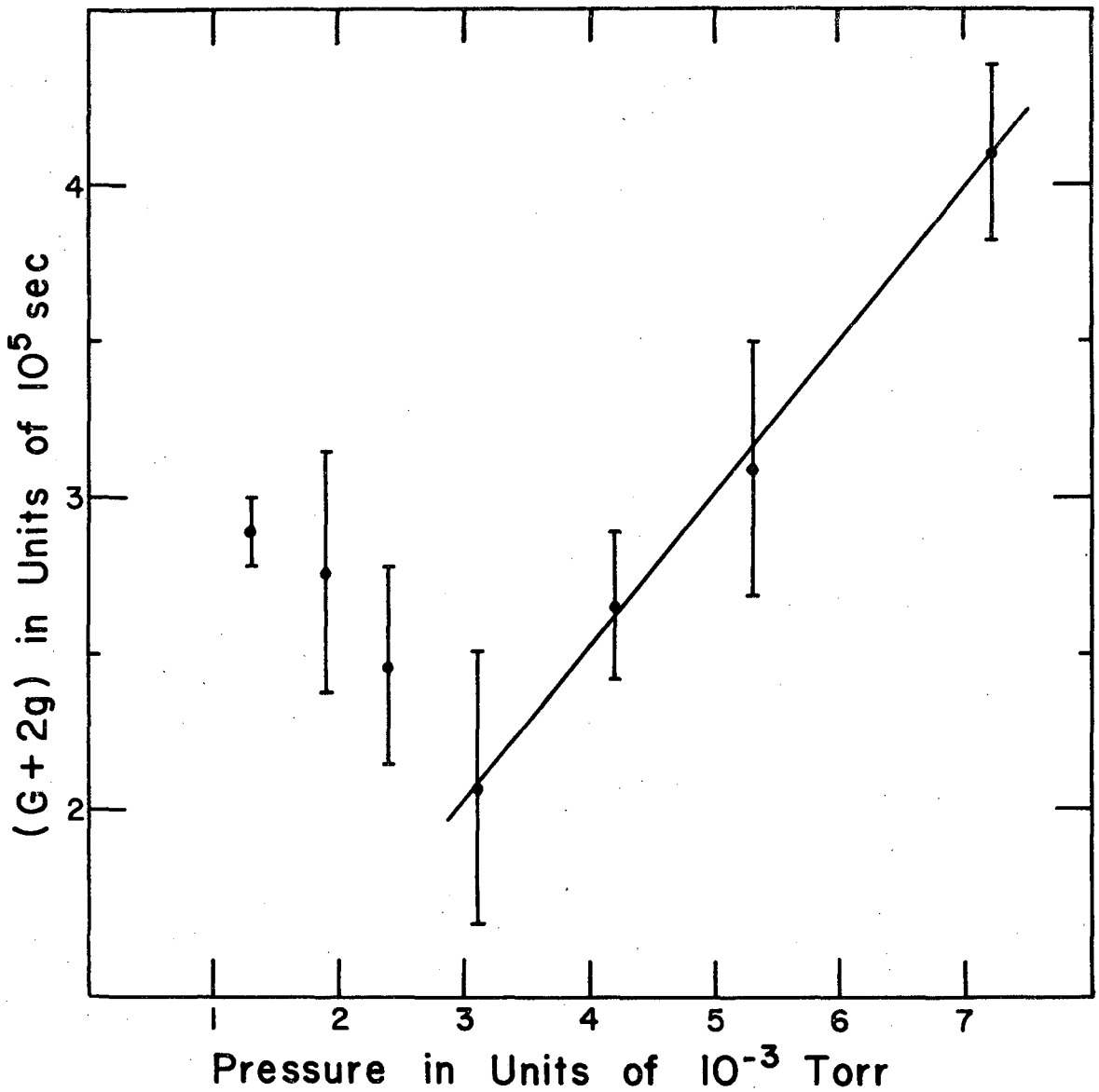

XBL 684-457

Fig. 20. (G+2g) as a function of pressure from the double-peaked resonances.

broaden the lines drastically. Baumann found a similar, though not so exaggerated, effect: Figure 21 is his graph of the extrapolated line widths he obtained.

The explanation that Baumann offers for this line broadening at low pressures is that the rf field is inhomogeneously distorted by the metal parts of the electron gun, that the movement of the metastable atoms within this inhomogeneous field should cause the resonance to be broadened as described by Millman,[26] and that this effect begins to take place as soon as the mean free path is long enough for the atoms to experience a considerable spatial variation in rf field strength within the m-state lifetime. It does not appear, however, that this is the genuine explanation. The effect that Millman describes is a broadening of an atomic beam resonance line due to an effective rf (slightly higher or lower than the applied frequency) experienced by the atoms as they pass through the ends of the rf hairpin, where the field is at right angles to the field in the main part of the hairpin. In both Baumann's experiment and this one the rf loops are circular and outside the electron gun so that a directly analogous situation cannot occur, and in addition the gun materials were deliberately chosen to be non-magnetic (the magnetic susceptibilities of molybdenum, tantalum, and tungsten are all less than 15×10^{-6}, in cgs units[27]), so there should be no distortion of the rf field on that account.

A more plausible reason for the particular shape of the line width-versus-pressure curve would be that the observed line width is actually the sum of line widths due to more than one kind of collision. If there

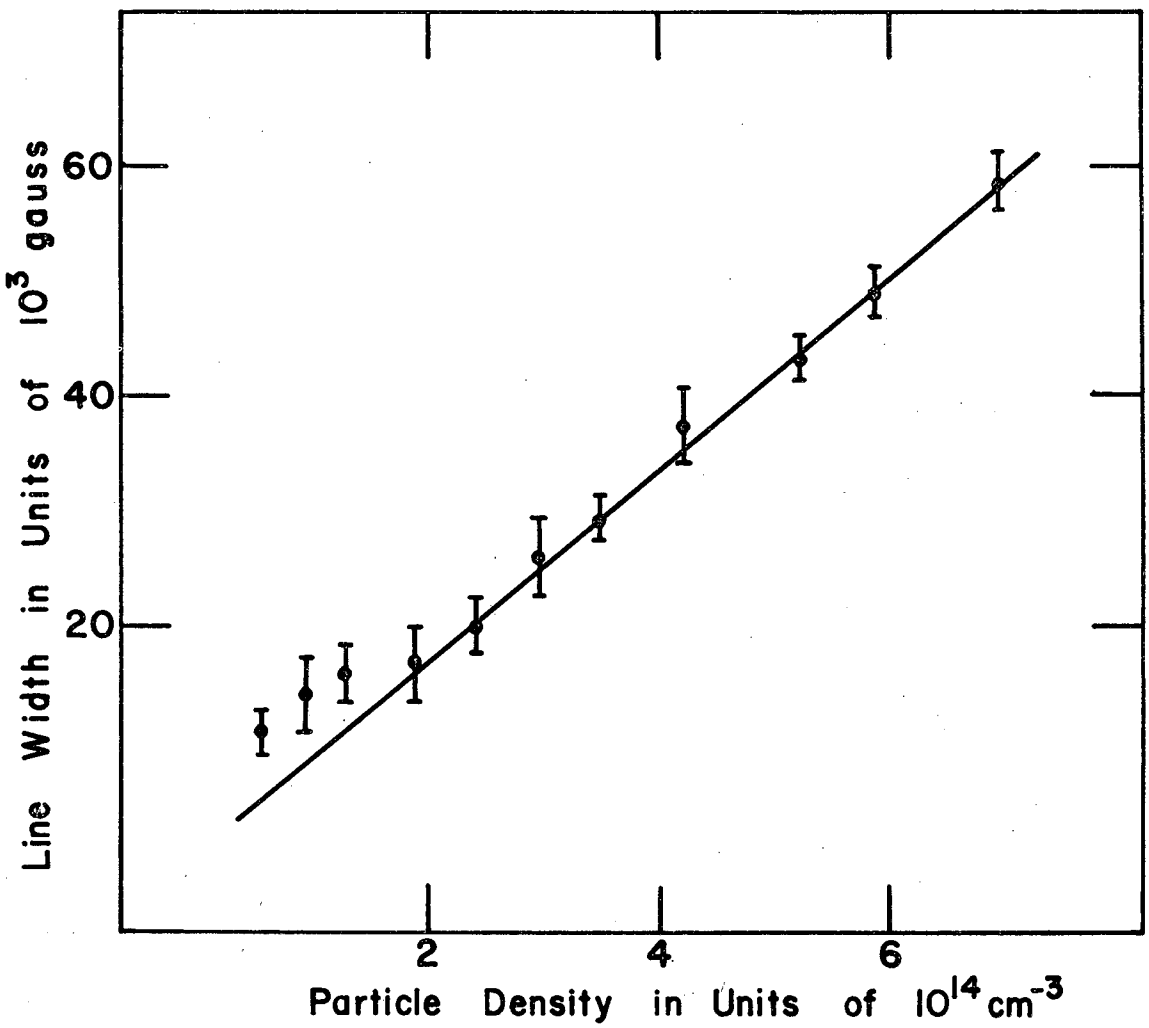

XBL 684-458

Fig. 21. A copy of a graph given by Baumann[7] showing resonance line widths (at zero rf field) as a function of the density of mercury atoms in his electron gun.

were only mercury atoms in the electron gun, there would be three species present in numbers great enough that they should be taken into consideration. These are ground state mercury atoms, mercury ions, and other metastable atoms.

The density of ground state atoms is equal to $\frac{1}{kT}$ times the pressure in the gun, minus the number of atoms excited to higher states. For the pressures used in this experiment and a temperature of 350° K, $\frac{p}{kT} = .36 - 2.0 \times 10^{14}$ atoms/cm^3. As we shall see, the number of ions and metastable atoms is small enough that subtracting their densities from this figure would make a negligible difference.

The number of ions may be estimated from several expressions derived by Langmuir[19] for plasmas such as existed in our electron gun. He gives for the number of ions/cm^3 at the edge of the plasma

$$n_p = \frac{1}{2}\sqrt{\frac{2\pi m_p}{kT_p}}\ \frac{I_s}{e} \quad ,$$

where m_p = mass of an ion, T_p = equivalent ion temperature, and I_s = ion current per area. If the ion concentration is fairly uniform, I_s is given by

$$I_s = I_e\sqrt{\frac{m_e}{m_p}} \quad ,$$

where I_e = electron current density, and $\frac{m_e}{m_p}$ = ratio of electron to ion masses. In order to estimate T_p, we may take 0.6 eV as a typical energy in a plasma of this kind; then T_p would be about 7000°. All this gives an $n_p \approx 2 \times 10^{10}$ ions/cm^3. Note that n_p should be independent of the pressure in the gun.

To get a rough estimate of the number of 6^3P_2 atoms, it is probably not unreasonable to use the cross section measured[28] for excitation to the 6^3P_2 state. This state is only about 0.6 eV lower, and it should have a similarly-shaped excitation function since it also is a triplet state. At an electron energy of 10 eV its excitation cross section is approximately 0.6×10^{-16} cm^2. With an electron flux of 4×10^{17} cm^{-2} sec^{-1} and a metastable state lifetime[7] of $1 - 3 \times 10^{-4}$ sec (depending on pressure), the number of metastable atoms should be

$$n_{met} = (n_{ground})(j_e)(\sigma_{ex})(\tau) \approx 10 \times 10^{10} \text{ cm}^{-3} - 14 \times 10^{11} \text{ cm}^{-3} .$$

Notice that since the lifetime of the metastable atoms depends on pressure (and in this region in fact rises approximately linearly with pressure), the only kind of mercury atoms with a density directly proportional to pressure are the ground state atoms. Thus it should follow logically that in the pressure region where the line width curve is linear, the metastable atoms are being disaligned by collisions with ground state atoms. The ground state is a $^1S_0$ state, however, and the question arises how it can have such a large effective collision cross section. At a pressure of 7.2×10^{-3} Torr, $\tau = .49 \times 10^{-5}$ sec and $n = 2.0 \times 10^{14}$ atoms/cm^3. For τ given by

$$\tau = \frac{1}{n\,\sigma\,v_{rel}} = \frac{1}{\sqrt{2}\,n\,\sigma\,\bar{v}} ,$$

$$\sigma = 3.8 \times 10^{-14} \text{ cm}^2$$

(at a temperature of 350° K, $\bar{v} = 1.9 \times 10^4$ cm sec). Either the ions, with a $^2S_{\frac{1}{2}}^{+}$ configuration, or the metastable atoms, with their $^3P_2$ configuration, would on the face of it be expected to have a larger

cross section than the spherical ground state atoms. (Notice, however, that in order to contribute to the lifetime, their cross sections would have to be considerably larger, on account of the 10^2-10^4 factor difference in densities.)

Most of the measurements that have been made of disorientation cross sections have involved collisions between two $^2S_{\frac{1}{2}}$ states[29] or between one $^1S_0$ state and one $^2S_{\frac{1}{2}}$ state[30], and the cross section for the latter is only of the order of 10^{-24} cm^2, although the former is up to 10^{-14} cm^2 because of spin exchange. Another kind of orienting or disorienting collision that has been investigated involves metastability exchange; i.e. the transfer of the energy of excitation between a metastable and a ground state. As has been pointed out[31], however, this process can change the orientation of the metastable atom only in the case of a non-zero nuclear spin and a degenerate ground state, and since we are concerned here with the even isotopes of mercury[32], those results do not apply.

Although the disorientation cross section is so small for a $^2S_{\frac{1}{2}}$ atom colliding with a $^1S_0$, the fact that the mercury metastable atoms are in a P state should make a great deal of difference. In fact, as Baumann points out, it is known[33] that a mercury 6^3P_2 atom will join with a $^1S_0$ ground state to form a shallowly bound molecule. This molecule is partly of a covalent and partly of a van der Waals type. Its van der Waals nature indicates that the atoms will retain their J quantization, but in the formation of the molecule the projections of their J values along the intermolecular axis become quantised and their

J vectors precess around that axis. Thus the J vector of the individual atom must change its orientation with respect to the external magnetic field. Since the dissociation energy of the molecule is only about 0.2 eV, the atoms composing it would soon separate, leaving the metastable atom with a definite probability of being in a new m state. Again because of the van der Waals nature of the molecule, the cross section for its formation should be rather large: the equilibrium separation of the two nuclei in the molecule must be about 2×10^{-8} cm [33,34], and the force between them should fall off only as r^{-6}, as opposed to the exponential decrease of a typical covalent bond.

Thus everything points to the ground state atoms as those responsible for the linear part of the line-width curve. The effect of the metastable atoms upon one another, although associated with relatively large cross sections, is probably not great enough to contribute significantly to the observed lifetime. Since J = 2 for the metastable state, one would expect an interaction between the magnetic dipoles of two $^3P_2$ states. A calculation along the lines of those of Byron and Foley[35] gives, however, a cross section of only about 3×10^{-16} cm^2, which, combined with a low density, is not enough to produce a τ of 10^{-5} sec.

The effect of the ions must also be considered. They could have a fairly large cross section for disaligning the metastable atoms, since electron exchange could turn the ion into a metastable atom with a new orientation. As mentioned above, however, their density should be dependent on the current in the electron gun, but more or less independent of the density of the mercury vapor. Thus one would expect their contribution to the line-width curve to be a flattening

out of the curve at pressures low enough that their density times cross section is very much greater than the density times respective cross section of the ground state atoms. Within the limits of error, and with the exception of the lowest-pressure point, this description could apply to the observed curve. If, however, the curve actually rises, as it seems to, at lower pressures, there may be still another process taking place.

A rise in line width at low pressures would suggest a localized source of disalignment which first would make its presence felt when the mean free path of the mercury atoms was long enough for a considerable number of them to enter the region and become affected. It has been mentioned that in spite of all precautions a blackening was observed on the wall of the electron gun in the neighborhood of the cathode. This means that there were in that region foreign particles, probably alumina molecules and their decomposition products, which had boiled off the insulation of the heater wire. These would tend to be large, polyatomic, and possibly charged molecules, which would be expected to have a very large cross section for disaligning the mercury metastable atoms.

It may be of interest to compare the various lifetime measurements. Baumann gives τ_m as a function of the density of mercury atoms in his electron gun rather than as a function of pressure, as we have been doing here, and he does not mention what the temperature in the gun would be, but it is possible to deduce his τ_m approximately as a function of pressure from his total pressure range, which he gives. His lower pressure results have been plotted in Fig. 22, together with the two present measurements of the lifetime. In comparing the present results

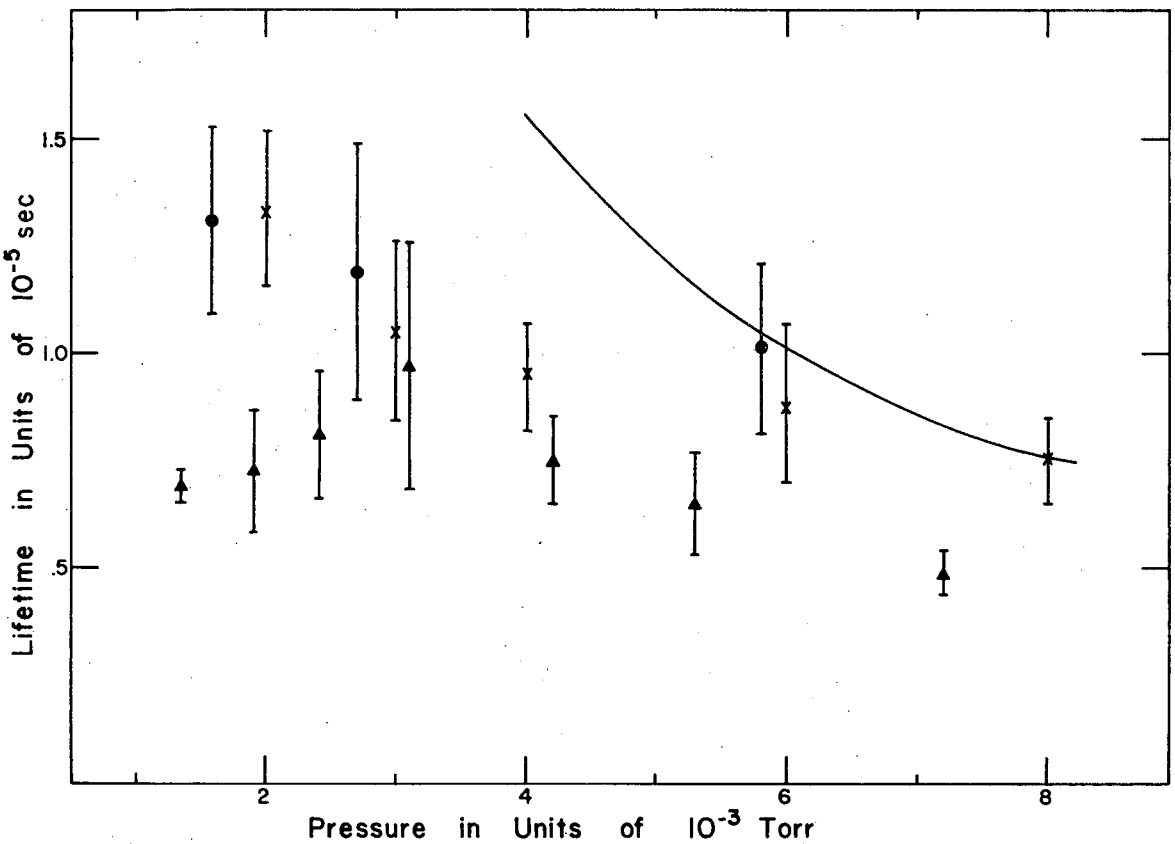

XBL 684-459

Fig. 22. The various measurements of τ_m. Baumann's results (approximated from his graph of lifetime versus particle density) are represented by crosses; the circles are the values of τ_m obtained here by the method of extrapolating the line width to zero rf field; and the triangles come from the measurements on the double-peaked resonance lines.

with those of Baumann it should be noted, however, that Baumann used the equation $\tau_m = 1/\Delta\omega$, whereas $\tau_m/2 = 1/\Delta\omega$ has been used here. According to our analysis, therefore, Baumann's values should all be multiplied by a factor of two. The upper curve in the graph corresponds approximately to Baumann's curve $\tau \propto 1/n$, which fits his higher pressure data (not shown here) very well and indicates again how the lower pressure points fail to follow the same relationship. That Baumann's τ_m's are (if multiplied by two) longer than those of the present measurements may be due to the larger electron gun current used here, 200 mA as opposed to Baumann's 20 mA. Both Baumann and Hadeishi and Liu[36] have found a significant line broadening with increasing electronic current, which may be due to the increasing number of ions present or may be due to the inhomogeneous magnetic field set up by the current.

V. CONCLUSION

It has been shown to be feasible to apply to neon the technique described in Section II, of using electron bombardment to produce and align an excited atomic state and of using optical detection of the rf resonance of that state. The g_J value of the metastable $(2^2P_{3/2}3^2S_{1/2})_2$ level of neon was obtained in this way in terms of the g_J value of the metastable 6^3P_2 level of mercury. A pronounced amplification of the resonance signal was obtained by adding a small amount of mercury vapor to the neon in the electron gun.

The equations for the neon and mercury resonance lines have been derived, taking into account all five magnetic sublevels of the J = 2 metastable states, and have been found to be the same except for a constant factor and a change of sign. The most significant feature of this equation is that it gives the half widths of the line as $1/\tau_J + 2/\tau_m$ instead of the more probable-appearing expression $1/\tau_J + 1/\tau_m$ (here τ_J is the lifetime of the metastable state as a whole, and τ_m is the lifetime of a particular m-level). Another somewhat surprising aspect of the equation is that it has the same form (substituting a different combination of τ's) as the corresponding equation for a J = 1 state. At first glance this would not be expected, since the equation comes from an integration over time of the Rabi-Majorana formula, which itself is different for different values of J and different initial and final m-states. The identical form of the equations comes from including as part of the J = 2 resonance all of the multiple quantum transitions that can affect it: these higher-order terms just cancel the higher-order terms that come

from the larger J value, with the result that, as stated, the J = 2 equation takes the same form as the J = 1 equation.

The lifetime of the metastable mercury m-states has been studied. It was measured by the usual method of graphing line widths squared versus rf power squared and extrapolating to zero rf field and was also obtained numerically from the separation of the double maxima in the strongly rf-broadened resonance line. The advantages of the latter method are that it avoids the problem of having to choose a baseline for the resonance, that the data collection time is shortened because it is not necessary to trace out the entire line, and that essentially every two (two because ratios were used) data points yields a value for the lifetime. This could be valuable in situations in which the resonance signal is weak or for which the lifetime is long enough that any reasonable rf power saturates the resonance.

The disadvantage of this method is that in order to avoid having to know the rf field exactly, ratios were taken of the expressions giving the relationship among the rf field, lifetime, and peak separation. These ratios are not linear with the lifetime term, however, and there were a number of data for which there was no numerical solution. A second combining of equations was required in order to be able to take into account all of the data. By this time the expression for the lifetime was fairly complicated, and, although it was still readily soluble by numerical methods, it may not seem as straightforward and appealing as the graphical approach in those situations for which the graphical method works well.

Baumann observed that at low pressures the lifetime dropped below the 1/p relationship to be expected of disalignment just by ground state atoms; the same thing occurred here also and was, in fact, quite exaggerated in the later measurements. The cause of this low-pressure line broadening may be the presence of foreign particles (probably from the heater wire insulation) in the neighborhood of the cathode; collisions with these would grow more important as the mean free path of the mercury atoms increased with decreasing pressure. In similar measurements in the future, precautions should be taken to eliminate the possibility of this contamination.

Another factor that could be improved in future measurements concerns the current in the electron gun. There have now been several observations that a large electronic current broadens the resonance line considerably; here it has been seen that Baumann's data, taken with a gun operated at 20 mA, indicate τ_m's that are definitely longer than those measured here, with a gun operated at 200 mA. The advantage of a larger current is, of course, that it produces more excited-state atoms. Thus, for the sake of efficiency, it may be desirable to take most of a set of data at a high current. Then, however, at least some of the measurements should be extrapolated back to zero or very small current in order to show where the true curve should lie.

ACKNOWLEDGMENTS

Many people taught and helped me in the course of this work. I should like to thank in particular:

Professor William A. Nierenberg, under whose direction most of the work was conducted;

Dr. Tetsuo Hadeishi, with whom and under whose direct supervision this project was accomplished;

Professor Howard A. Shugart, for his interest and for his direction during the last part of this work;

Professor Richard Marrus, for his guidance in the first part of my graduate career;

Mr. Douglas B. MacDonald, for his help with a number of mechanical problems and with the vacuum system in particular;

Mr. Wilton A. Berlund, for the many electron guns and much glassware he constructed;

Mr. Michiyuki Nakamura and Mr. Marvin Hartley for the benefit of their electronic knowledge and skills;

Mrs. Julia Taylor for typing this thesis and for kindly tending to many last-minute duties for me after I had left California.

This work was supported by the U. S. Atomic Energy Commission.

APPENDICES

I. Alignment Due to Cascading

Radiative transitions to the J = 2 state can take place from any higher state with J = 1, 2, or 3. The matrix element for the transition is proportional to $\langle J'=2,m'|\vec{r}|J,m\rangle$. Writing $\vec{r} = rC_1^1 + rC_0^1 + rC_{-1}^1$ [where, as usual, $C_q^k = \sqrt{\frac{4\pi}{2k+1}}\, Y_{kq}(\theta,\phi)$], we find that the relative transition probabilities to any m' are given by

$$\left|\langle J'=2\|rC^1\|J\rangle\right|^2 \left\{ n_{m'-1}(J)\left|\begin{pmatrix} 2 & 1 & J \\ -m' & 1 & m'-1 \end{pmatrix}\right|^2 + n_{m'}(J)\left|\begin{pmatrix} 2 & 1 & J \\ -m' & 0 & m' \end{pmatrix}\right|^2 + n_{m'+1}(J)\left|\begin{pmatrix} 2 & 1 & J \\ -m' & -1 & m'+1 \end{pmatrix}\right|^2 \right\}$$

$$= \frac{\left|\langle J'=2\|rC^1\|J\rangle\right|^2}{2J+1} \left\{ n_{m'-1}(J)\left|(2\ -m'\ 1\ 1|2\ 1\ J\ 1-m')\right|^2 + n_{m'}(J)\left|(2\ -m'\ 1\ 0|2\ 1\ J\ -m')\right|^2 + n_{m'+1}(J)\left|(2\ -m'\ 1\ -1|2\ 1\ J\ -m'-1)\right|^2 \right\},$$

where $n_m(J)$ is the number of atoms in the state J,m. Keeping only the m dependence we have, then,

$$n_2(^3P_2) \propto n_1(J)\left|(2\ -2\ 1\ 1|2\ 1\ J\ -1)\right|^2 + n_2(J)\left|(2\ -2\ 1\ 0|2\ 1\ J\ -2)\right|^2 + n_3(J)\left|(2\ -2\ 1\ -1|2\ 1\ J\ -3)\right|^2$$

$$n_1(^3P_2) \propto n_0(J)\left|(2\ -1\ 1\ 1|2\ 1\ J\ 0\right|^2 + n_1(J)\left|(2\ -1\ 1\ 0|2\ 1\ J\ -1)\right|^2 + n_2(J)\left|(2\ -1\ 1\ -1|2\ 1\ J\ -2\right|^2$$

$$n_0(^2P_2) \propto n_0(J)\left|(2\ 0\ 1\ 0|2\ 1\ J\ 0)\right|^2 + 2n_1(J)\left|(2\ 0\ 1\ -1|2\ 1\ J\ -1)\right|^2$$

When the three possible values of J are inserted and the Clebsch-Gordan coefficients evaluated (see, for example, Table 5.2 in A. R. Edmonds' Angular Momentum in Quantum Mechanics), the relative populations are given by the following:

from $J = 3$, $n_2(^3P_2) \propto \frac{1}{15} n_1(J) + \frac{1}{3} n_2(J) + n_3(J) = n_{-2}(^3P_2)$

$$n_1(^3P_2) \propto \frac{1}{5} n_0(J) + \frac{8}{15} n_1(J) + \frac{2}{3} n_2(J) = n_{-1}(^3P_2)$$

$$n_0(^3P_2) \propto \frac{3}{5} n_0(J) + \frac{4}{5} n_1(J)$$

from $J = 2$, $n_2(^3P_2) \propto \frac{1}{3} n_1(J) + \frac{2}{3} n_2(J) = n_{-2}(^3P_2)$

$$n_1(^3P_2) \propto \frac{1}{2} n_0(J) + \frac{1}{6} n_1(J) + \frac{1}{3} n_2(J) = n_{-1}(^3P_2)$$

$$n_0(^3P_2) \propto n_1(J) \text{ , and}$$

from $J = 1$, $n_2(^3P_2) \propto \frac{3}{5} n_1(J) = n_{-2}(^3P_2)$

$$n_1(^3P_2) \propto \frac{3}{10} n_0(J) + \frac{3}{10} n_1(J) = n_{-1}(^3P_2)$$

$$n_0(^3P_2) \propto \frac{2}{5} n_0(J) + \frac{1}{5} n_1(J) \quad .$$

Since the initial J,m state was created by low-energy electron bombardment in the z direction, the $m = 0$ and, by electron exchange and each to a lesser extent, the $m = \pm 1$ substates should be the more heavily populated; thus it is clear that cascading transitions to the $^3P_2$ state will tend to align it also. In fact, it can be seen that even if the initial m-state populations are all equal, radiative transitions to the metastable state will still partially align it.

II. The Motion of the Expectation Value of the Magnetic Moment μ

(See, for example, reference 37.)

For a total magnetic field of

$$\vec{H}(t) = \hat{i}H_r \cos \omega_z t + \hat{j}H_r \sin \omega_z t + \hat{k}H_z$$

the Schrödinger equation is

$$\frac{-\hbar}{i} \frac{\partial\psi}{\partial t} = -\vec{\mu}\cdot\vec{H}\,\psi$$
$$= -\gamma\hbar[H_r(J_x \cos \omega_z t + J_y \sin \omega_z t) + H_z J_z]\psi \ .$$

This is the same thing as

$$\frac{-\hbar}{i} \frac{\partial\psi}{\partial t} = -\gamma\hbar\left[H_r\left(e^{-i\omega_z t J_z} J_x e^{i\omega_z t J_z}\right) + H_z J_z\right]\psi$$

since J_z generates rotations of the coordinate system in the positive z direction. As in the classical case, the problem can be simplified by going to a rotating coordinate system; i.e. by setting $\psi = e^{-i\omega_z t J_z}\psi'$, where ψ' is the wave function in the rotating system. Then

$$\frac{-\hbar}{i}\frac{\partial\psi'}{\partial t} = -\gamma\hbar\left[H_r J_x + \left(H_z + \frac{\omega_z}{\gamma}\right) J_z\right]\psi' \ . \quad \text{Also}$$
$$\psi'(t) = e^{\frac{-i}{\hbar}\mathcal{H}' t}\psi'(0) \ ,$$

where $\mathcal{H}'$ is the Hamiltonian, $-\hbar[\gamma H_r J_x + (\gamma H_z + \omega_z)J_z]$, in the rotating coordinate system. Thus the wave function in the laboratory coordinates is

$$\psi(t) = e^{-i\omega_z t J_z} e^{\frac{-i}{\hbar}\mathcal{H}' t}\psi'(0)$$
$$= e^{-i\omega_z t J_z} e^{\frac{-i}{\hbar}\mathcal{H}' t}\psi(0) \ , \text{ and}$$

$$\langle\mu_z(t)\rangle = \gamma\hbar\int\psi(t)^* J_z\psi(t)\, d\tau \ .$$

This is, in general, a very complicated expression, since $\mathcal{H}'$ contains non-commuting operators, which are now in the exponents. Exactly at resonance the J_z term in $\mathcal{H}'$ is zero, however, and in this case the motion of μ is given by

$$\langle\mu_z(t)\rangle = \gamma\hbar\int\psi^*(0)\, e^{\frac{it}{\hbar}(-\hbar\gamma H_r J_x)}\, e^{i\omega_z t J_z}\, J_z\, e^{-i\omega_z t J_z}\, e^{-\frac{it}{\hbar}(-\hbar\gamma H_r J_x)}\psi(0)d\tau$$

$$= \gamma\hbar\int\psi^*(0)\, e^{-it\gamma H_r J_x}\, J_z\, e^{it\gamma H_r J_x}\,\psi(0)d\tau \quad .$$

But J_x generates rotations of the coordinate system in the positive x direction, so this is the same as

$$\langle\mu_z(t)\rangle = \gamma\hbar\int\psi^*(0)\,[J_z\cos\gamma H_r t - J_y\sin\gamma H_r t]\psi(0)d\tau \ .$$

Therefore

$$\langle\mu_z(t)\rangle = \langle\mu_z(0)\rangle\cos\gamma H_r t - \langle\mu_y(0)\rangle\sin\gamma H_r t \quad .$$

FOOTNOTES AND REFERENCES

[1] H. G. Dehmelt, Phys. Rev. 103, 1125 (1956).

[2] W. E. Lamb, Jr., Phys. Rev. 105, 559 (1956).

[3] W. E. Lamb, Jr., and T. H. Maiman, Phys. Rev. 105, 573 (1956).

[4] T. Hadeishi, Ph.D. thesis, Lawrence Radiation Laboratory Report UCRL-10477 (1962).

[5] T. Hadeishi, O. A. McHarris, and W. A. Nierenberg, Bull. Am. Phys. Soc. 9, 625 (1964).

[6] T. Hadeishi, O. A. McHarris, and W. A. Nierenberg, Phys. Rev. 138, A983 (1965).

[7] M. Baumann, Z. Physik 173, 519 (1963).

[8] J. R. Oppenheimer, Z. Physik 43, 27 (1927).

[9] H. A. Bethe, Handbuch der Physik (Springer Verlag Berlin 1933), Vol. 24, pp. 508-515.

[10] See, for example, reference 2.

[11] I. I. Rabi, Phys. Rev. 51, 652 (1937).

[12] I. I. Rabi, N. F. Ramsey, and J. Schwinger, Rev. Mod. Phys. 26, 167 (1954).

[13] N. F. Ramsey, Molecular Beams (Oxford at the Clarendon Press 1956).

[14] E. Majorana, Nuovo Cimento 9, 43 (1932).

[15] J. Brossel and F. Bitter, Phys. Rev. 86, 308 (1952).

[16] F. Bitter and J. Brossel, Technical Report No. 176, Massachusetts Institute of Technology Research Laboratory of Electronics (1950).

[17] For a general reference see F. Rosebury, Handbook of Electron Tube and Vacuum Techniques (Addison-Wesley 1965).

[18] J. R. Pierce, Theory and Design of Electron Beams (Van Nostrand 1954).

[19] I. Langmuir, Phys. Rev. 33, 954 (1929).

[20] R. Bock, Z. Physik 54, 257 (1929).

[21] Mc Dermott and Lichten, Phys. Rev. 119, 134 (1960).

[22] Lurio, Weinreich, Drake, Hughes, and White, Phys. Rev. 120, 153 (1960).

[23] In order to see that wall collisions are not important here, note that $v_{RMS} = 2.1 \times 10^4$ cm/sec for a temperature of about 350° K inside the electron gun. A mercury atom travels, then, about 2.1 mm in a lifetime of 10^{-5} sec, and an aligned atom initially even at the outside edge of the interaction region is at least six times this distance from the wall of the tube.

[24] H. Margenau and G. M. Murphy, The Mathematics of Physics and Chemistry (D. Van Nostrand Co, Inc. 1956).

[25] Handbook of Chemistry and Physics (Chemical Rubber Co. 1965-66) p. D-96.

[26] S. Millman, Phys. Rev 55, 628 (1939).

[27] Handbook of Chemistry and Physics (Chemical Rubber Co. 1965-66) pp. E-97, E-99.

[28] H. M. Jongerius, Philips Res. Rep. Suppl. No. 2 (1962) as reported by D. W. O. Heddle and M. J. Seaton in Atomic Collision Processes (North-Holland Publishing Co., Amsterdam, 1964) p. 139.

[29] See, for example, S. M. Jarrett, Phys. Rev. 133, A111 (1964).

[30] For a discussion see R. M. Herman, Phys. Rev. 136, A1576 (1964).

[31] F. D. Colegrove, L. D. Schearer, and G. K. Walters, Phys. Rev. 132, 2561 (1963).

[32] To see that Zeeman resonances of the odd isotopes are not involved, consider the field H at which the closest odd-isotope resonance would occur (which would be that for Hg^{199}, I = 1/2, F = 3/2, g_F = 9/5):

$$H_{even} - H_{odd} = \frac{h\nu}{\mu_0}\left(\frac{1}{g_J} - \frac{1}{g_F}\right)$$

$$= \frac{h\nu}{\mu_0}\left(\frac{2}{3} - \frac{5}{9}\right) = \frac{1}{9}\frac{h\nu}{\mu_0}$$

Compare this to a typical experimental curve:

$$H_{even} = \frac{h\nu}{\mu_0}\frac{1}{g_J} \geq 3.5 \text{ gauss} .$$

Thus $H_{even} - H_{odd} \geq \frac{3.5}{6}$ gauss, which would be well off the edge of any of our graphs.

[33] W. Finkelnburg, Kontinuierliche Spektren (Springer 1938).

[34] G. Hertzberg, Spectra of Diatomic Molecules (D. Van Nostrand Co., Inc. 1950).

[35] F. W. Byron, Jr., and H. M. Foley, Phys. Rev. 134A, 625 (1964).

[36] T. Hadeishi and C.-H. Liu, Phys. Rev. Letters 16, 1035 (1966).

[37] C. P. Slichter, Principles of Magnetic Resonance (Harper and Row 1963).

This report was prepared as an account of Government sponsored work. Neither the United States, nor the Commission, nor any person acting on behalf of the Commission:

A. Makes any warranty or representation, expressed or implied, with respect to the accuracy, completeness, or usefulness of the information contained in this report, or that the use of any information, apparatus, method, or process disclosed in this report may not infringe privately owned rights; or

B. Assumes any liabilities with respect to the use of, or for damages resulting from the use of any information, apparatus, method, or process disclosed in this report.

As used in the above, "person acting on behalf of the Commission" includes any employee or contractor of the Commission, or employee of such contractor, to the extent that such employee or contractor of the Commission, or employee of such contractor prepares, disseminates, or provides access to, any information pursuant to his employment or contract with the Commission, or his employment with such contractor.